

*Application
for
United States Letters Patent*

To all whom it may concern:

Be it known that **David M. Stern and Shi Du Yan**

have invented certain new and useful improvements in

**Transgenic Mice Over-Expressing ABAD and Mutant APP in Brain as Model of Alzheimer's Disease
And Uses Thereof**

of which the following is a full, clear and exact description.

Transgenic Mice Over-expressing ABAD and Mutant APP in
Brain as Model of Alzheimer's Disease and Uses Thereof

5

The invention disclosed herein was made with Government support under Grant No. AG16736 from the National Institute on Aging in the National Institutes of Health of the U.S. Department of Public Health. Accordingly, the U.S. Government has certain rights in this invention.

Background of the Invention

15

Throughout this application, various publications are referenced by number. Full citations for these publications may be found listed at the end of the specification immediately preceding the claims. The disclosures of these publications in their entireties are hereby incorporated by reference into this application in order to more fully describe the state of the art as known to those skilled therein as of the date of the invention described and claimed herein.

The pain of Alzheimer's disease results directly from the memory loss and cognitive deficits suffered by the patient. These eventually result in the patient's loss of identity, autonomy, and freedom. As a step toward curing this disease, alleviating its symptoms, or retarding its progression, it would be desirable to develop a transgenic animal model exhibiting the main debilitating phenotype of Alzheimer's disease, that is, memory loss, expressed concomitantly with the neuropathological correlates of Alzheimer's disease, for example, beta-amyloid accumulation, increased glial reactivity, and hippocampal cell loss.

It is estimated that over 5% of the U.S. population over 65 and over 15% of the U.S. population over 85 are beset with some form of Alzheimer's disease (Cross, A. J., Eur J Pharmacol (1982) 82:77-80; Terry, R. D., et al., Ann Neurol 5 (1983) 14:497-506). It is believed that the principal cause for confinement of the elderly in long term care facilities is due to this disease, and approximately 65% of those dying in skilled nursing facilities suffer from it.

10 Certain facts about the biochemical and metabolic phenomena associated with the presence of Alzheimer's disease are known. Two morphological and histopathological changes noted in Alzheimer's disease brains are neurofibrillary tangles (NFT) and amyloid deposits. Intraneuronal neurofibrillary
15 tangles are present in other degenerative diseases as well, but the presence of amyloid deposits both in the interneuronal spaces (neuritic plaques) and in the surrounding microvasculature (vascular plaques) seems to be characteristic of Alzheimer's. Of these, the neuritic plaques
20 seem to be the most prevalent (Price, D. L., et al., Drug Development Research (1985) 5:59-68). Plaques are also seen in the brains of aged Down's Syndrome patients who develop Alzheimer's disease.

Summary of the Invention

The present invention provides for a transgenic non-human animal whose cells contain a DNA sequence comprising: (a) a nerve tissue specific promoter operatively linked to a DNA sequence which encodes amyloid-beta peptide alcohol dehydrogenase (ABAD), and (b) a nerve tissue specific promoter operatively linked to a DNA sequence encoding a mutant human amyloid precursor protein hAPP695, hAPP751 and hAPP770 bearing mutations linked to familial Alzheimer's disease in humans, wherein said non-human animal exhibits at least one phenotype from the group consisting of: reduced basal synaptic transmission; inhibited synaptic plasticity; increased neuronal stress; elevated 4-hydroxynonenal in cerebral cortex; increased heme oxygenase type I in cerebral cortex; decreased synaptophysin in cerebral cortex; decreased microtubule-associated protein 2 in cerebral cortex; and increased levels of activated caspase 3 antigen in cortical neurons.

Brief Description of the Figures

Figures 1A-1B. Schematic depiction of strategy for making Tg PD-ABAD mice. Figure 1A: entire construct; Figure 1B: transgenic cassette for microinjection.

Figure 2. Southern analysis of three founders for Tg PD-ABAD mice: lanes 1-3 show mice positive for the transgene and lanes 4-6 are nontransgenic littermates.

10

Figure 3. Identification of Tg PD-ABAD mice (+) and nontransgenic littermate controls (-) by PCR.

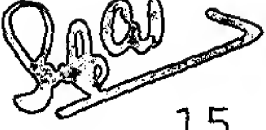
 **Figures 4A, 4B, 4C and 4D.** ABAD expression in Tg PD-ABAD mice (+) compared with nontransgenic littermate controls (-). Figure 4A (Northern) and Figure 4B (Western) analysis of homogenates of cerebral cortex. Equal amounts of RNA (note approximately equal intensity of 28S ribosomal RNA band on the ethidium bromide stained gel) and protein were loaded in each lane. Figures 4C-4D show immunohistochemical identification of RAGE in cerebral cortex from a Tg PD-RAGE mouse (Figure 4C) and a nontransgenic littermate control (Figure 4D).

Figure 5. RAGE expression in brain subregions of Tg PD-ABAD mice compared with nontransgenic littermate controls (nonTg). Immunoblotting was performed protein extracts of brain homogenates derived from the indicated brain subregion.

Figures 6A-6C. The effect of ABAD overexpression on the proton-decoupled ^{13}C NMR spectra of freeze-clamped brain after perfusion with D-[2,4- ^{13}C] β -hydroxybutyrate. Figure 6A. The spectrum from a representative Tg PD-ABAD mouse

displays prominent glutamate and glutamine peaks. The inset shows expanded regions of resonances of glutamate (G-4), glutamine (GL-4) and GABA (GA-2) from Tg (PD-ABAD) mice. Abbreviations: G-2, G-3, and G-4 denote the position 2, 3, and 4 carbons of glutamate, respectively; GL-2, GL-3 and GL-4 denote the position 2, 3 and 4 carbons of glutamine, respectively; and, GA-2 corresponds to C-2 of GABA. Figure 6B. The effect of ABAD overexpression on areas of glutamate C-4 resonance in brain extracts of Tg PD-ABAD and nonTg littermate control mice as obtained from ^{13}C - NMR analysis. Values are expressed as the ratio of the area of the glutamate C-4 peak over the area of an added standard acetate (see Methods). *Glutamate and glutamine levels were significantly higher in Tg PD-ABAD mice than in nonTg controls ($P < 0.03$; $N = 4$, in each case). Total areas of ^{13}C -glutamate (G-2 + G-3 + G-4) were significantly higher in the Tg PD-ABAD compared with nonTG littermate controls. Figure 6C. Basal ATP levels in whole brain extracts from Tg PD-ABAD ($N = 5$) or nonTg littermate controls ($N = 5$) were measured as described in the text. Animals were fasted overnight, and the brain was removed and freeze-clamped for ATP and β -hydroxybutyrate (BHB) analysis. * indicates $P < 0.03$. In each case, the data is reported as the mean \pm SD.

25 **Figures 7A-7D.** Induction of stroke in Tg PD-ABAD mice. Figures 7A-7B. Tg PD-ABAD mice and nonTg littermates were subjected to middle cerebral artery occlusion and were evaluated 24 hrs after the ischemic insult to determine neurologic deficit score (Figure 7B), and, following sacrifice, infarct volume (Figure 7A). Figures 7C-7D. At 30 the same time point, cerebral cortex was harvested to determine ATP, lactate and β -hydroxybutyrate (BHB) levels determined on extracts of whole brains (from animals

subjected to the stroke procedure 24 hrs previously) from Tg PD-ABAD or nonTg control mice (N=5, in each case). Data is reported as the mean \pm SD ($P < 0.04$ for ATP and $P < 0.03$ for lactate). Transient middle cerebral artery occlusion model of stroke in mice: comparison of infarct volume in Tg PD-RAGE and nontransgenic littermate controls (nonTg). * $P < 0.05$.

Figure 8. Identification of a double transgenic mouse overexpressing ABAD and mutant human APP by PCR.

10

Figures 9A-E. Expression of 4-hydroxynonenal-lysine epitopes in cerebral cortex from double Tg mice overexpressing ABAD and mutant human APP (hAPP) termed Tg PD-ABAD/hAPP. Figures 9A-9D demonstrate immunocytochemistry of representative sections and the far right panel (Figure 9E) shows quantitation of immunocytochemical results from multiple fields of all mice in each of the experimental groups.

Figures 10A-10E. Increased expression of heme oxygenase (HO)-1 in cerebral cortex from double Tg mice overexpressing ABAD and mutant human APP (hAPP). Figure 10A, Northern analysis for HO-1 transcripts. Figures 10B-10D, immunostaining for HO-1 antigen. Figure 10E, Quantitation of immunocytochemical results from multiple fields of all mice in each of the experimental groups.

Figures 11A-11B. Semiquantitative analysis of synaptophysin immunoreactivity in hippocampus of Tg PD-RAGE/hAPP, Tg PD-RAGE, Tg hAPP, and nontransgenic littermate control mice at 4 months of age.

Figures 12A1, 12A2, 12A3, 12A4, and 12B. Increased expression of activated caspase-3 in cerebral cortex from Tg

PD-RAGE/hAPP mice. Figures 12A1-12A4, immunostaining for activated caspase-3. Figure 12B, quantitation of immunocytochemical results from multiple fields of all mice in each of the experimental groups. Scale bar, 10 μ m.

5

Figures 13A-13B. Northern analysis (Figure 13A) and immunoblotting (Figure 13B) of E16 cortical neuron cultures with 32 P-labelled human ABAD cDNA (Figure 13A) or anti-human RAGE IgG (Figure 13B). (+) indicates neurons obtained from

10 Tg PD-RAGE mice and (-) indicates neurons are from nontransgenic littermate controls.

Detailed Description of the Invention

The present invention provides for a transgenic non-human animal whose cells contain a DNA sequence comprising: (a) a
5 nerve tissue specific promoter operatively linked to a DNA
sequence which encodes amyloid-beta peptide alcohol
dehydrogenase (ABAD), and (b) a nerve tissue specific
promoter operatively linked to a DNA sequence encoding a
10 mutant human amyloid precursor protein hAPP695, hAPP751 and
hAPP770 bearing mutations linked to familial Alzheimer's
disease in humans, wherein said non-human animal exhibits at
least one phenotype from the group consisting of: reduced
basal synaptic transmission; inhibited synaptic plasticity;
increased neuronal stress; elevated 4-hydroxynonenal in
15 cerebral cortex; increased heme oxygenase type I in cerebral
cortex; decreased synaptophysin in cerebral cortex; decreased
microtubule-associated protein 2 in cerebral cortex; and
increased levels of activated caspase 3 antigen in cortical
neurons.

20
The present invention also provides for a method for
evaluating in a non-human transgenic animal the potential
therapeutic effect of an agent for treating Alzheimer's
disease in a human, which comprises: (a) providing an agent
25 to a transgenic non-human animal whose cells comprise (i) a
nerve tissue specific promoter operatively linked to a DNA
sequence which encodes amyloid-beta peptide alcohol
dehydrogenase (ABAD), and (ii) a nerve tissue specific
promoter operatively linked to a DNA sequence encoding a
30 mutant human amyloid precursor protein hAPP695, hAPP751 and
hAPP770 bearing mutations linked to familial Alzheimer's
disease, (b) determining the therapeutic effect of the agent
on the transgenic non-human animal by monitoring basal

synaptic transmission or synaptic plasticity, wherein an increase in basal synaptic transmission or synaptic plasticity indicates that the agent would have a potential therapeutic effect on Alzheimer's disease in a human.

5

In one embodiment of the invention, the promoter of both element (a) and (b) is platelet derived growth factor (PDGF)-B-chain promoter.

- 10 In another embodiment of the invention, the non-human animal is a mouse, a rat, a sheep, a dog, a primate, or a reptile. In another embodiment, the animal is a mammal.

The sequences for mutant APP and for ABAD are publically
15 available in the GenBank. For example, several sequences of ABAD obtained from the GenBank are recited below:

LOCUS HCD2_RAT 261 aa ROD 30-MAY-2000

DEFINITION 3-HYDROXYACYL-COA DEHYDROGENASE TYPE II (TYPE II
HADH) (ENDOPLASMIC RETICULUM-ASSOCIATED AMYLOID BETA-PEPTIDE
20 BINDING PROTEIN).

ACCESSION O70351PID g7387724

VERSION O70351 GI:7387724DB

SOURCE swissprot: locus HCD2_RAT, accession O70351; class: standard. created: May
30, 2000. sequence updated: May 30, 2000. annotation updated: May 30, 2000. xrefs: gi:
25 2961552, gi: 2961553 xrefs (non-sequence databases): HSSP P19992, PFAM PF00106,
PROSITE PS00061KEYWORDS Oxidoreductase; NAD; Acetylation.

SOURCE Norway rat. ORGANISM Rattus norvegicus Eukaryota; Metazoa; Chordata;
Craniata; Vertebrata; Euteleostomi; Mammalia; Eutheria; Rodentia; Sciurognathi;
Muridae; Murinae; Rattus.

30 REFERENCE 1 (residues 1 to 261)

AUTHORS Gunn-Moore,F.J. and Tavare,J.M. TITLE Direct Submission

JOURNAL Submitted (??-FEB-1998) to the EMBL/GenBank/DDBJ databases

REMARK SEQUENCE FROM N.A. TISSUE=LIVERCOMMENT

[CATALYTIC ACTIVITY] L-3-HYDROXYACYL-COA + NAD(+) = 3-OXOACYL-COA + NADH. [SUBUNIT] TETRAMER (BY SIMILARITY). [SUBCELLULAR
5 LOCATION] MITOCHONDRIAL (BY SIMILARITY). [SIMILARITY] BELONGS TO
THE SHORT-CHAIN DEHYDROGENASES/REDUCTASES (SDR)
FAMILY.FEATURES Location/Qualifiers source 1..261 /organism="Rattus norvegicus"
/db_xref="taxon:10116" 1..261 Protein 1..261 /product="3-HYDROXYACYL-COA
DEHYDROGENASE TYPE II" /EC_number="1.1.1.35" Site 2 /site_type="acetylation"
10 /note="(BY SIMILARITY)." Site 12..37 /site_type="np-binding" /note="NAD (BY
SIMILARITY)." Site 168 /site_type="active" /note="BY SIMILARITY."

ORIGIN

1 maaavrsvkg lvavitggas glglstakrl vgqgataavl dvpnsegete akklggncif
15 61 apanvtseke vqaaltlake kfgridvavn cagiavaikt yhekknqvht ledfqrvinv
121 nligtnvir lvagvmgqne pdqggqrgvi intasvaafe gqvgqaaysa skggivgmtl
181 piardlapig irvvtiapgl fatpllttlp dkvrnflasq vpfpsrlgdp aeyahlvqmv
241 ienpflngev irldgairmq p// (SEQ ID NO:1)

20

LOCUS AF035555 973 bp mRNA PRI 07-MAY-1998

DEFINITION Homo sapiens short chain L-3-hydroxyacyl-CoA dehydrogenase (SCHAD)
mRNA, complete cds.

ACCESSION AF035555

25 VERSION AF035555.1 GI:3116433

KEYWORDS

.SOURCE human.

ORGANISM Homo sapiens Eukaryota; Metazoa; Chordata; Craniata; Vertebrata;
Euteleostomi; Mammalia; Eutheria; Primates; Catarrhini; Hominidae; Homo.

30

REFERENCE 1 (bases 1 to 973)

AUTHORS He,X.Y., Schulz,H. and Yang,S.Y.

TITLE A human brain L-3-hydroxyacyl-coenzyme A dehydrogenase is identical to an amyloid beta-peptide-binding protein involved in Alzheimer's disease

JOURNAL J. Biol. Chem. 273 (17), 10741-10746 (1998)

5 MEDLINE 98221216

REFERENCE 2 (bases 1 to 973)

AUTHORS Yang,S.-Y., Schulz,H. and He,X.-Y.

TITLE Direct Submission

JOURNAL Submitted (21-NOV-1997) Pharmacology, Institute for Basic Research in

10 Developmental Disabilities, 1050 Forest Hill Road, Staten Island, NY 10314,

USAFEATURES Location/Qualifiers source 1..973 /organism="Homo sapiens"

/db_xref="taxon:9606" /chromosome="X" /map="Xp11.21" /cell_type="neuron"

/tissue_type="brain" gene 1..973 /gene="SCHAD" CDS 25..810 /gene="SCHAD"

/EC_number="1.1.1.35" /note="fatty acid beta-oxidation enzyme" /codon_start=1

15 /product="short chain L-3-hydroxyacyl-CoA dehydrogenase" /protein_id="AAC15902.1"

/db_xref="GI:3116434" /translation="

MAAACRSVKGLVAVITGGASGLGLATAERLVGQGASAVLLDLPN

SGGEAQAKKLGNNCVFAPADV TSEKDVQTALALAKGKFGRVDVAVNCAGIAVASKTYN

20 LKKGQTHLTLEDFQRVLDVNLMTFNVIRLVAGEMQNEPDQGGQRGVIINTASVAAFE

GQVGQAAYSASKGGIVGMTLP IARDLAPIGIRVMTIAPGLFGTPLLTS LPEKVCNFLA

SQVPFPSRLGDP AEY AHLVQAI IENPFLNGEVIRLDGAIRMQP (SEQ ID NO:2)

BASE COUNT 222 a 262 c 287 g 202 t

25

ORIGIN

1 tcccgtggag tggccggcga caagatggca gcagcgtgtc ggagcgtgaa gggcctggtg 61 gcggtataaa

ccggaggagc ctcgggcctg ggcctggcca cggcggagcg acttgtgggg 121 cagggagcct ctgctgtgct

tctggacctg cccaactcgg gtggggaggc ccaagccaag 181 aagttaggaa acaactgcgt ttgcggccca

30 gccgacgtga cctctgagaa ggatgtgcaa 241 acagctctgg ctctagcaaa aggaaagttt ggccgtgtgg

atgtagctgt caactgtgca 301 ggcatcgcgg tggctagcaa gacgtacaac ttaaagaagg gccagaccca

taccttgaa 361 gacttcagc gagttcttga tgtgaatctc atgggcacct tcaatgtgat ccgcctggtg 421

gctggtgaga tgggccagaa tgaaccagac cagggaggcc aacgtggggt catcatcaac 481 actgccagt

tggtgcctt cgagggcag gttggacaag ctgcatactc tgcttccaag 541 gggggaatag tgggcatgac
actgcccatt gctcgggatc tggctcccat aggtatccgg 601 gtgatgacca ttgcccagg tctgtttggc
acccactgc tgaccagcct ccagagaaa 661 gtgtgcaact tcttgccag ccaagtgcc ttccctagcc
gactgggtga ccctgctgag 721 tatgtcacc tcgtacagge catcatcgag aaccattcc tcaatggaga
5 ggtcatcgg 781 ctggatgggg ccattcgtat gcagcctga agggagaagg cagagaaaac acacgtcct 841
ctgcccttcc ttccctggg gtactactct ccagtcttg gaggaagccc agtagccatt 901 ttgtaactgc ctaccagtcg
ccctctgtgc ctaataaagt ctcttttct cacagaaaaa 961 aaaaaaaaaa aaa// (SEQ ID NO:3)

Definitions

10

"DNA sequence" is a linear sequence comprised of any combination of the four DNA monomers, i.e., nucleotides of adenine, guanine, cytosine and thymine, which codes for genetic information, such as a code for an amino acid, a promoter, a control or a gene product. A specific DNA sequence is one which has a known specific function, e.g., codes for a particular polypeptide, a particular genetic trait or affects the expression of a particular phenotype.

15

20 "Genotype" is the genetic constitution of an organism.

"Phenotype" is a collection of morphological, physiological and biochemical traits possessed by a cell or organism that results from the interaction of the genotype and the environment.

25

"Phenotypic expression" is the expression of the code of a DNA sequence or sequences which results in the production of a product, e.g., a polypeptide or protein, or alters the expression of the zygote's or the organisms natural phenotype.

30

"Zygote" is a diploid cell having the potential for

development into a complete organism. The zygote can result from parthenogenesis, nuclear transplantation, the merger of two gametes by artificial or natural fertilization or any other method which creates a diploid cell having the potential for development into a complete organism. The origin of the zygote can be from either the plant or animal kingdom.

In the practice of any of the methods of the invention or preparation of any of the pharmaceutical compositions an "therapeutically effective amount" is an amount which is capable of alleviating the symptoms of the disorder of memory or learning in the subject. Accordingly, the effective amount will vary with the subject being treated, as well as the condition to be treated. For the purposes of this invention, the methods of administration are to include, but are not limited to, administration cutaneously, subcutaneously, intravenously, parenterally, orally, topically, or by aerosol.

By "nervous system-specific" is meant that expression of a nucleic acid sequence occurs substantially in a nervous system tissue (for example, the brain or spinal cord). Preferably, the expression of the nucleic acid sequence in the nervous system tissue represents at least a 5-fold, more preferably, a 10-fold, and, most preferably, a 100-fold increase over expression in non-nervous system tissue.

The "non-human animals" of the invention include vertebrates such as rodents, non-human primates, sheep, dog, cow, amphibians, reptiles, etc. Preferred non-human animals are selected from the rodent family including rat and mouse, most preferably mouse.

The "transgenic non-human animals" of the invention are produced by introducing "transgenes" into the germline of the non-human animal.

5 Advantages of the present invention

Fig 4

10 The transgenic non-human mammals of the present invention will provide insights with respect to how and where protein interactions occur in Alzheimer's Disease and thus provide more useful models for testing the efficacy of certain drugs in preventing or reducing the onset or progression of this disease. The transgenic non-human mammals of the present invention include recombinant genetic material comprised of a nucleic acid sequence encoding RAGE fused to specific
15 promoters capable of expressing the protein in specific tissues such as nerve tissues generally and/or specific types of nerve tissue, e.g., the brain.

20 As described herein, the current invention provides a number of advantages. First, because transgenic animals are generally useful for the investigation of specific biological processes and for reproducing particular aspects of human disease, the transgenic animals of the invention provide an important, reproducible and accurate means for screening
25 drugs to isolate therapeutic agents. In particular, the transgenic animals that are described for the first time herein have the advantage of mimicking the cognitive defects observed in patients with Alzheimer's disease. Accordingly, the efficacy of a particular therapy may be examined in the
30 same animal at different disease stages. Importantly, because this invention provides a transgenic animal model of Alzheimer's disease with measurable phenotypes, compounds may be screened to identify those which alleviate this symptom,

even absent knowledge of the symptom's underlying biological cause.

In addition, although not strictly required for drug
5 screening, the associated neuro-pathological symptoms
exhibited by the transgenic animal models described herein
provide the unique advantage of allowing the investigation
of the etiology of Alzheimer's disease. For example, the
appearance of reduced synaptic plasticity or the reduced
10 basal synaptic transmission may be correlated with the
appearance of specific behavioral impairments within
individuals or groups of animals. In addition, treatments
which are shown to improve memory function may be tested for
their ability to selectively improve certain pathological
15 symptoms.

Another advantage of this invention is the ease with which
these transgenic animals are bred to produce identical
transgenic progeny. The animals of the invention may be
20 generated in sufficient quantity to make them widely and
rapidly available to researchers in this field.

Further Detailed Description of the Invention

The present invention also provides for a transgenic nonhuman animal whose germ or somatic cells contain a nucleic acid molecule which comprises: (a) a nerve tissue specific promoter operatively linked to a DNA sequence which encodes amyloid-beta peptide alcohol dehydrogenase (ABAD), and (b) a nerve tissue specific promoter operatively linked to a DNA sequence encoding a mutant human amyloid precursor protein hAPP695, hAPP751 and hAPP770 bearing mutations linked to familial Alzheimer's disease in humans, introduced into the mammal, or an ancestor thereof, at an embryonic stage.

This transgenic animal may be used in screening methods for compounds which would be useful in the treatment of neurological disorders in humans. A method for screening compounds for their potential use as therapeutic agents which comprises administering to the transgenic non-human mammal described herein the compound, in various amounts, and observing whether the neurological function of the transgenic mammal improves or not (as determined by, for example, basal synaptic transmission, synaptic plasticity, neuronal stress, et al.).

The neurological disorder may be amnesia, Alzheimer's disease, amyotrophic lateral sclerosis, a brain injury, cerebral senility, chronic peripheral neuropathy, a cognitive disability, a degenerative disorder associated with learning, Down's Syndrome, dyslexia, electric shock induced amnesia or amnesia. Guillain-Barre syndrome, head trauma, Huntington's disease, a learning disability, a memory deficiency, memory loss, a mental illness, mental retardation, memory or cognitive dysfunction, multi-infarct

dementia and senile dementia, myasthenia gravis, a neuromuscular disorder, Parkinson's disease, Pick's disease, a reduction in spatial memory retention, senility, or Turret's syndrome.

5

The compound which is tested in the screening method of the present invention may be an organic compound, a nucleic acid, a small molecule, an inorganic compound, a lipid, or a synthetic compound. The mammal may be a mouse, a sheep, a
10 bovine, a canine, a porcine, or a primate. The administration may comprise intralesional, intraperitoneal, intramuscular or intravenous injection; infusion; liposome-mediated delivery; gene bombardment; topical, nasal, oral, anal, ocular or otic delivery.

15

The present invention also provides for a method for alleviating symptoms in a subject suffering from a neurological disorder which comprises administering to the subject an effective amount of the compound evaluated by the
20 methods hereinabove in an amount effective to treat the symptoms in the subject suffering from a neurological disorder.

The administration may be intralesional, intraperitoneal,
25 intramuscular or intravenous injection; infusion; liposome-mediated delivery; gene bombardment; topical, nasal, oral, anal, ocular or otic delivery.

Pharmaceutical compositions and Carriers

30

As used herein, the term "suitable pharmaceutically acceptable carrier" encompasses any of the standard pharmaceutically accepted carriers, such as phosphate

buffered saline solution, water, emulsions such as an oil/water emulsion or a triglyceride emulsion, various types of wetting agents, tablets, coated tablets and capsules. An example of an acceptable triglyceride emulsion useful in intravenous and intraperitoneal administration of the compounds is the triglyceride emulsion commercially known as Intralipid®.

Typically such carriers contain excipients such as starch, milk, sugar, certain types of clay, gelatin, stearic acid, talc, vegetable fats or oils, gums, glycols, or other known excipients. Such carriers may also include flavor and color additives or other ingredients.

15 This invention also provides for pharmaceutical compositions including therapeutically effective amounts of protein compositions and compounds together with suitable diluents, preservatives, solubilizers, emulsifiers, adjuvants and/or carriers useful in treatment of neuronal degradation due to aging, a learning disability, or a neurological disorder. Such compositions are liquids or lyophilized or otherwise dried formulations and include diluents of various buffer content (e.g., Tris-HCl., acetate, phosphate), pH and ionic strength, additives such as albumin or gelatin to prevent absorption to surfaces, detergents (e.g., Tween 20, Tween 80, Pluronic F68, bile acid salts), solubilizing agents (e.g., glycerol, polyethylene glycerol), anti-oxidants (e.g., ascorbic acid, sodium metabisulfite), preservatives (e.g., Thimerosal, benzyl alcohol, parabens), bulking substances or tonicity modifiers (e.g., lactose, mannitol), covalent attachment of polymers such as polyethylene glycol to the compound, complexation with metal ions, or incorporation of the compound into or onto particulate preparations of

polymeric compounds such as polylactic acid, polglycolic acid, hydrogels, etc, or onto liposomes, micro emulsions, micelles, unilamellar or multi lamellar vesicles, erythrocyte ghosts, or spheroplasts. Such compositions will influence
5 the physical state, solubility, stability, rate of in vivo release, and rate of in vivo clearance of the compound or composition. The choice of compositions will depend on the physical and chemical properties of the compound.

10 Controlled or sustained release compositions include formulation in lipophilic depots (e.g., fatty acids, waxes, oils). Also comprehended by the invention are particulate compositions coated with polymers (e.g., poloxamers or poloxamines) and the compound coupled to antibodies directed
15 against tissue-specific receptors, ligands or antigens or coupled to ligands of tissue-specific receptors. Other embodiments of the compositions of the invention incorporate particulate forms protective coatings, protease inhibitors or permeation enhancers for various routes of administration,
20 including parenteral, pulmonary, nasal and oral.

Portions of the compound of the invention may be "labeled" by association with a detectable marker substance (e.g., radiolabeled with ^{125}I or biotinylated) to provide reagents
25 useful in detection and quantification of compound or its receptor bearing cells or its derivatives in solid tissue and fluid samples such as blood, cerebral spinal fluid or urine.

When administered, compounds are often cleared rapidly from
30 the circulation and may therefore elicit relatively short-lived pharmacological activity. Consequently, frequent injections of relatively large doses of bioactive compounds may be required to sustain therapeutic efficacy. Compounds

modified by the covalent attachment of water-soluble polymers such as polyethylene glycol, copolymers of polyethylene glycol and polypropylene glycol, carboxymethyl cellulose, dextran, polyvinyl alcohol, polyvinylpyrrolidone or polyproline are known to exhibit substantially longer half-lives in blood following intravenous injection than do the corresponding unmodified compounds (Abuchowski et al., 1981; Newmark et al., 1982; and Katre et al., 1987). Such modifications may also increase the compound's solubility in aqueous solution, eliminate aggregation, enhance the physical and chemical stability of the compound, and greatly reduce the immunogenicity and reactivity of the compound. As a result, the desired in vivo biological activity may be achieved by the administration of such polymer-compound adducts less frequently or in lower doses than with the unmodified compound.

Attachment of polyethylene glycol (PEG) to compounds is particularly useful because PEG has very low toxicity in mammals (Carpenter et al., 1971). For example, a PEG adduct of adenosine deaminase was approved in the United States for use in humans for the treatment of severe combined immunodeficiency syndrome. A second advantage afforded by the conjugation of PEG is that of effectively reducing the immunogenicity and antigenicity of heterologous compounds. For example, a PEG adduct of a human protein might be useful for the treatment of disease in other mammalian species without the risk of triggering a severe immune response. The compound of the present invention capable of alleviating symptoms of a cognitive disorder of memory or learning may be delivered in a microencapsulation device so as to reduce or prevent an host immune response against the compound or against cells which may produce the compound. The compound

of the present invention may also be delivered microencapsulated in a membrane, such as a liposome.

5 Polymers such as PEG may be conveniently attached to one or more reactive amino acid residues in a protein such as the alpha-amino group of the amino terminal amino acid, the epsilon amino groups of lysine side chains, the sulfhydryl groups of cysteine side chains, the carboxyl groups of aspartyl and glutamyl side chains, the alpha-carboxyl group
10 of the carboxy-terminal amino acid, tyrosine side chains, or to activated derivatives of glycosyl chains attached to certain asparagine, serine or threonine residues.

15 Numerous activated forms of PEG suitable for direct reaction with proteins have been described. Useful PEG reagents for reaction with protein amino groups include active esters of carboxylic acid or carbonate derivatives, particularly those in which the leaving groups are N-hydroxysuccinimide, p-nitrophenol, imidazole or 1-hydroxy-2-nitrobenzene-4-
20 sulfonate. PEG derivatives containing maleimido or haloacetyl groups are useful reagents for the modification of protein free sulfhydryl groups. Likewise, PEG reagents containing amino hydrazine or hydrazide groups are useful for reaction with aldehydes generated by periodate oxidation of
25 carbohydrate groups in proteins.

In one embodiment the compound of the present invention is associated with a pharmaceutical carrier which includes a pharmaceutical composition. The pharmaceutical carrier may
30 be a liquid and the pharmaceutical composition would be in the form of a solution. In another embodiment, the pharmaceutically acceptable carrier is a solid and the composition is in the form of a powder or tablet. In a

further embodiment, the pharmaceutical carrier is a gel and the composition is in the form of a suppository or cream. In a further embodiment the active ingredient may be formulated as a part of a pharmaceutically acceptable
5 transdermal patch.

Transgenic Technology and Methods

The following U.S. Patents are hereby incorporated by
10 reference: U.S. Patent No. 6,025,539, IL-5 transgenic mouse; U.S. Patent No. 6,023,010, Transgenic non-human animals depleted in a mature lymphocytic cell-type; U.S. Patent No. 6,018,098, In vivo and in vitro model of cutaneous photoaging; U.S. Patent No. 6,018,097, Transgenic mice
15 expressing human insulin; U.S. Patent No. 6,008,434, Growth differentiation factor-11 transgenic mice; U.S. Patent No. 6,002,066; H2-M modified transgenic mice; U.S. Patent No. 5,994,618, Growth differentiation factor-8 transgenic mice; U.S. Patent No. 5,986,171, Method for examining
20 neurovirulence of polio virus, U.S. Patent No. 5,981,830, Knockout mice and their progeny with a disrupted hepsin gene; U.S. Patent No. 5,981,829, .DELTA.Nur77 transgenic mouse; U.S. Patent No. 5,936,138; Gene encoding mutant L3T4 protein which facilitates HIV infection and transgenic mouse
25 expressing such protein; U.S. Patent No. 5,912,411, Mice transgenic for a tetracycline-inducible transcriptional activator; U.S. Patent No. 5,894,078, Transgenic mouse expressing C-100 app.

30 The methods used for generating transgenic mice are well known to one of skill in the art. For example, one may use the manual entitled "Manipulating the Mouse Embryo" by Brigid Hogan et al. (Ed. Cold Spring Harbor Laboratory) 1986.

See for example, Leder and Stewart, U.S. Patent No. 4,736,866 for methods for the production of a transgenic mouse.

5 For sometime it has been known that it is possible to carry out the genetic transformation of a zygote (and the embryo and mature organism which result therefrom) by the placing or insertion of exogenous genetic material into the nucleus of the zygote or to any nucleic genetic material which
10 ultimately forms a part of the nucleus of the zygote. The genotype of the zygote and the organism which results from a zygote will include the genotype of the exogenous genetic material. Additionally, the inclusion of exogenous genetic material in the zygote will result in a phenotype expression
15 of the exogenous genetic material.

The genotype of the exogenous genetic material is expressed upon the cellular division of the zygote. However, the phenotype expression, e.g., the production of a protein
20 product or products of the exogenous genetic material, or alterations of the zygote's or organism's natural phenotype, will occur at that point of the zygote's or organism's development during which the particular exogenous genetic material is active. Alterations of the expression of the
25 phenotype include an enhancement or diminution in the expression of a phenotype or an alteration in the promotion and/or control of a phenotype, including the addition of a new promoter and/or controller or supplementation of an existing promoter and/or controller of the phenotype.

30

The genetic transformation of various types of organisms is disclosed and described in detail in U.S. Pat. No. 4,873,191, issued Oct. 10, 1989, which is incorporated herein by

reference to disclose methods of producing transgenic organisms. The genetic transformation of organisms can be used as an in vivo analysis of gene expression during differentiation and in the elimination or diminution of genetic diseases by either gene therapy or by using a transgenic non-human mammal as a model system of a human disease. This model system can be used to test putative drugs for their potential therapeutic value in humans.

- 10 The exogenous genetic material can be placed in the nucleus of a mature egg. It is preferred that the egg be in a fertilized or activated (by parthenogenesis) state. After the addition of the exogenous genetic material, a complementary haploid set of chromosomes (e.g., a sperm cell or polar body) is added to enable the formation of a zygote. The zygote is allowed to develop into an organism such as by implanting it in a pseudopregnant female. The resulting organism is analyzed for the integration of the exogenous genetic material. If positive integration is determined, the organism can be used for the in vivo analysis of the gene expression, which expression is believed to be related to a particular genetic disease.

Attempts have been made to study a number of different types of genetic diseases utilizing such transgenic animals. Attempts related to studying Alzheimer's disease are disclosed within published PCT application WO89/06689 and PCT application WO89/06693, both published on Jul. 27, 1989, which published applications are incorporated herein by reference to disclose genetic sequences coding for Alzheimer's .beta.-amyloid protein and the incorporation of such sequences into the genome of transgenic animals.

Embryonal target cells at various developmental stages can be used to introduce transgenes. Different methods are used depending on the stage of development of the embryonal target cell. The zygote is the best target for micro-injection. In the mouse, the male pronucleus reaches the size of approximately 20 micrometers in diameter which allows reproducible injection of 1-2 pl of DNA solution. The use of zygotes as a target for gene transfer has a major advantage in that in most cases the injected DNA will be incorporated into the host gene before the first cleavage (Brinster, et al. (1985) Proc. Natl. Acad. Sci. U.S.A. 82, 4438-4442). As a consequence, all cells of the transgenic non-human animal will carry the incorporated transgene. This will in general also be reflected in the efficient transmission of the transgene to offspring of the founder since 50% of the germ cells will harbor the transgene. Microinjection of zygotes is the preferred method for incorporating transgenes in practicing the invention.

Retroviral infection can also be used to introduce transgene into a non-human animal. The developing non-human embryo can be cultured in vitro to the blastocyst stage. During this time, the blastomeres can be targets for retroviral infection (Jaenich, R. (1976) Proc. Natl. Acad. Sci U.S.A. 73, 1260-1264). Efficient infection of the blastomeres is obtained by enzymatic treatment to remove the zona pellucida (Hogan, et al. (1986) in Manipulating the Mouse Embryo, Cold Spring Harbor Laboratory Press, Cold Spring Harbor, N.Y.). The viral vector system used to introduce the transgene is typically a replication-defective retrovirus carrying the transgene (Jahner, et al. (1985) Proc. Natl. Acad. Sci. U.S.A. 82, 6927-6931; Van der Putten, et al. (1985) Proc. Natl. Acad. Sci U.S.A. 82, 6148-6152). Transfection is easily and

efficiently obtained by culturing the blastomeres on a monolayer of virus-producing cells (Van der Putten, supra; Stewart, et al. (1987) EMBO J. 6, 383-388). Alternatively, infection can be performed at a later stage. Virus or virus-producing cells can be injected into the blastocoele (Jahner, D., et al. (1982) Nature 298, 623-628). Most of the founders will be mosaic for the transgene since incorporation occurs only in a subset of the cells which formed the transgenic non-human animal. Further, the founder may contain various retroviral insertions of the transgene at different positions in the genome which generally will segregate in the offspring. In addition, it is also possible to introduce transgenes into the germ line, albeit with low efficiency, by intrauterine retroviral infection of the midgestation embryo (Jahner, D. et al. (1982) supra).

A third type of target cell for transgene introduction is the embryonal stem cell (ES). ES cells are obtained from pre-implantation embryos cultured in vitro and fused with embryos (Evans, M. J., et al. (1981) Nature 292, 154-156; Bradley, M. O., et al. (1984) Nature 309, 255-258; Gossler, et al. (1986) Proc. Natl. Acad. Sci U.S.A. 83, 9065-9069; and Robertson, et al. (1986) Nature 322, 445-448). Transgenes can be efficiently introduced into the ES cells by DNA transfection or by retrovirus-mediated transduction. Such transformed ES cells can thereafter be combined with blastocysts from a non-human animal. The ES cells thereafter colonize the embryo and contribute to the germ line of the resulting chimeric animal. For review see Jaenisch, R. (1988) Science 240, 1468-1474.

As used herein, a "transgene" is a DNA sequence introduced into the germline of a non-human animal by way of human

intervention such as by way of the above described methods.

The disclosures of publications referenced in this application in their entirety are hereby incorporated by
5 reference into this application in order to more fully describe the state of the art as known to those skilled therein as of the date of the invention described and claimed herein.

10 This invention is illustrated in the Experimental Details section which follows. These sections are set forth to aid in an understanding of the invention but are not intended to, and should not be construed to, limit in any way the invention as set forth in the claims which follow thereafter.

15

20170324 09:55:11

EXPERIMENTAL DETAILS

Example 1: Generation of Transgenic Mice With Targeted Overexpression of Amyloid-beta peptide alcohol dehydrogenase (ABAD) in Neurons

This section describes a means of making transgenic mice with targeted overexpression of ABAD in neurons using the PDGF B-chain promoter and the cDNA for human full-length ABAD. The mice, termed "Tg PD-ABAD," which have been produced provide a model system for determining the consequences of heightened ABAD expression in neurons, and could serve as an important model system to test ABAD inhibitors. Cross-breeding of Tg PD-ABAD mice with other animals, such as those expressing a transgene causing overexpression of mutant amyloid precursor protein (resulting in increased production of amyloid-beta peptide) provide a model system to assess the effects of ABAD in an A β -rich environment in the brain relevant to Alzheimer's disease. In addition, isolation and culture of embryonic neurons from Tg PD-ABAD mice allows study of the consequences of increased levels of ABAD *in vitro* in actual neurons. These are several examples of how Tg PD-ABAD mice can be used to assess the contribution of ABAD, analyzed according to *in vitro* and *in vivo* systems, to situations potentially relevant to human disease.

Introduction

Amyloid-beta peptide alcohol dehydrogenase (ABAD) is a member of the short-chain dehydrogenase reductase family of oxidoreductases¹⁻⁶. ABAD is present in endoplasmic reticulum and mitochondria^{1,3}. It shares in common with other members of the family cofactor binding sites (in this case for NAD[H]) and a Rossmann fold. However, it appears to be unique

in its ability to bind amyloid-beta peptide (A β) and to utilize a range of substrates, including hydroxyacyl Coenzyme A adducts, β -hydroxybutyrate, alcohols and steroids (17 β -estradiol etc)^{2,4-6}. Possible physiologic roles for ABAD are suggested by the lethal phenotype observed on inactivation of *scully*, the *Drosophila* counterpart, which is associated with multiple developmental abnormalities⁷. However, in an A β -rich environment, ABAD appears to switch from a physiologic to a pathogenic role. In cultured cell systems, overexpression of ABAD appears to confer increased sensitivity to the toxic effects of A β ^{1,2}. For example, COS or neuroblastoma cells overexpressing APP(V717G) when cotransfected to overexpress ABAD display exaggerated cell stress based on generation of reactive aldehydes (malondialdehyde and 4-hydroxynonenal; HNE), and increased DNA fragmentation². Taken together with the increased levels of ABAD in neurons in the brains of patients with Alzheimer's disease (AD), this has led us to speculate that ABAD might be an important cofactor for A β -induced cell stress. Furthermore, from its location in the endoplasmic reticulum it could potentially interact with nascent A β allowing it to participate in pathogenesis at early times.

This section demonstrates the production of mice overexpressing ABAD in neurons under control of the PDGF B-chain promoter. The resulting transgenic mice have several evident uses: 1) a model for demonstrating the consequences of increased ABAD expression in neurons (as in response to ischemic stress, though this could be extended to inflammatory and other stimuli); 2) a model for testing the effect of inhibitors of ABAD (at the level of the enzyme's active site, determinants mediating interaction with A β , or

other critical portions of the molecule); 3) a source of cultures for primary cortical neurons overexpressing ABAD (which could be used to test inhibitors); and, 4) a starting point for cross-breeding studies to produce double-transgenic mice (for example, cross-breeding with mice overexpressing the hAPP transgene which results in increased generation of A β ; the double transgenic mice resulting from such a cross display increased levels of ABAD in an A β -rich environment).

10 Methods

Construction of the transgene and making the transgenic (Tg) mice. The platelet-derived growth factor (PDGF) B-chain promoter was used to drive overexpression of ABAD in neurons of the central nervous system of transgenic (Tg) mice⁸. Transgene constructs were prepared using a previously described vector^{9,10}. Briefly, the CMV immediate/early promoter was excised from the commercial expression vector pCI (Promega, Madison WI), and replaced with an oligonucleotide polylinker. The PDGF B-chain promoter fragment was mobilized as an XbaI fragment⁸ and cloned into a unique SpeI site designed within the synthetic linker. The full-length human ABAD cDNA was inserted into the NotI site of the original polylinker. A schematic representation of this construct is shown in **Fig. 1A**. An \approx 3 kb fragment containing the promoter, cDNA and required other sequences was then excised from the plasmid backbone as a PvuI fragment (**Fig. 1B**) and microinjected mouse B6CBAF₁/J oocytes. The latter were implanted into pseudopregnant females and mated with B6CBAF₁/J males resulting in the generation of independent founders. Breeding of these mice demonstrated germ-line transmission and was used to produce lines of animals termed Tg PD-ABAD.

Founders were initially identified by Southern blotting performed on DNA extracted from mouse tails. DNA was digested, run on agarose gels, and hybridized with ³²P-labelled cDNA for human ABAD. Tails were digested with
5 proteinase K (500 µg/ml) in digestion buffer (50 mM Tris, pH 8.0, 100 mM EDTA, 0.5% SDS) at 55°C for overnight. Then, purified DNA was cleaved with EcoRI overnight at 37°C. Labelling of the probe was done using the Stratagene's Probe Labeling Kit™. Autoradiography was then performed.

10

Subsequent screening of progeny was by PCR using the following primers: 5'-GGCAGCAGCGTGTCGGAGCG-3' (SEQ ID NO:4) and 3'-AGGGCAGAGGAGCGTGTGT-5' (SEQ ID NO:5). Total RNA was isolated using Trizol®, and RT-PCR was performed with the
15 following thermocycling parameters: 30 sec for each cycle consisting of incubations at 95°C for 20 sec, 57°C for 30 sec and 72°C for 1 sec for a total of 35 cycles. Products were analyzed by agarose gel electrophoresis (1%) and visualized by ethidium bromide staining under ultraviolet illumination.
20 The size of the ABAD amplicon with these primers corresponded to 821 bp.

Northern and immunoblotting utilized the same procedures as above, except that tissue was homogenized in the presence of
25 Trizol (RNA) or in homogenization buffer (Tris/HCl, 10 mM, pH 7.4; NaCl, 100 mM; phenylmethanesulfonylfluoride, 100 µg/ml; EDTA, 1 mM; aprotinin, 1 µg/ml). Note that immunoblotting and immunostaining of brain tissue from Tg PD-ABAD mice used anti-human ABAD peptide IgG which appears to
30 be preferentially immunoreactive with human ABAD, the latter encoded by the transgene.

Characterization of ABAD expression in Tg PD-ABAD mice.

Northern analysis was performed on total RNA isolated from cerebral cortex, hippocampus and cerebellum. RNA was isolated using Trizol[®] followed by electrophoresis on 0.8% agarose gels (30 μ g was applied to each lane), transfer to nitrocellulose membranes, and hybridization with ³²P-labelled human ABAD cDNA. The ABAD cDNA was labelled by as above.

10 Western blotting was performed on protein extracts of brain subregions. Proteins were extracted from minced pieces of brains by exposing the tissue to lysis buffer (Tris/HCl, 20 mM; pH 7.4; Triton X-100, 1%; phenylmethylsulfonylfluoride, 2 mM; EDTA, 1 mM, aprotinin, 10 μ g/ml; leupeptin, 10 μ g/ml) using a ratio of 1 ml of buffer per 0.5 gm of tissue.

15 Extracts were then boiled in reducing SDS-sample buffer, and applied to SDS-PAGE (12%) according to Laemmli¹¹. Antibody to recombinant human ABAD was employed as described²

Immunostaining was performed on paraformaldehyde (4%)-fixed, paraffin embedded sections (6 μ m) of mouse brains prepared according to standard methods^{12,13}. The sections were deparaffinized and dehydrated, and then stained with rabbit anti-human ABAD IgG (50 μ g/ml) followed by goat anti-rabbit biotin-conjugated IgG and ExtrAvidin-conjugated with alkaline phosphatase (Biotin ExtrAvidin[®] kit; Sigma, St. Louis MO).

25 Preparation of anti-ABAD IgG, using recombinant ABAD as the immunogen, has been described².

30 Cross-breeding of Tg PD-RAGE mice with Tg hAPP mice. Tg mice overexpressing an alternatively spliced hAPP minigene that encodes hAPP695, hAPP751, and hAPP770 bearing mutations linked to familial AD (V717F, K670M/N671L) have been produced by Dr. Lennart Mucke¹⁴, and provided to us for use in cross-

breeding studies with Tg PD-RAGE mice. In these mice, expression of the transgene is also driven by the PDGF B-chain promoter. Cross-breeding was performed and double-transgenic mice expressing both hAPP and PD-ABAD transgenes were identified with specific primers. The primers for the hAPP transgene were: 5'-GACAAGTATCTCGAGACACCTGGGGATGAG-3' (SEQ ID NO:6) and 3'-AAAGAACTTGTAGGTTGGATTTTCGTACC-5' (SEQ ID NO:7). PCR conditions for the amplifying the hAPP transgene were the same as those described above, and the size of the amplicon was 1169 bp.

Characterization of Tg PD-ABAD/hAPP mice. Mice were anesthetized according to standard procedures and then flush-perfused transcardially with solution containing NaCl (0.9%). Brains will then be rapidly removed and divided sagittally. One hemibrain was postfixed in phosphate-buffered saline (PBS) containing paraformaldehyde (4%; pH 7.4) at 4°C for 48 hrs prior to vibratome sectioning. Hemibrains were stored in cryoprotectant medium (phosphate-buffered saline containing glycerin and ethylene glycol) until sectioning. This portion of the brain was employed for studies of neuronal integrity and degeneration. There is ample evidence that loss of synaptophysin-immunoreactivity in presynaptic terminals is associated with AD brain, a marker which correlates with extent of cognitive impairments¹⁵⁻²⁰. Additionally, immunoreactivity for Microtubule-associated protein (MAP)-2 was examined as a marker of neuronal cell bodies and dendrites, as a significant decrease of MAP-2 immunoreactive dendrites has been observed for example, in brains of patients with neurodegeneration subsequent to HIV-1 encephalitis²¹.

Hemibrains were subjected to sagittal sectioning employing

a Leica Vibratome 1000E. Sections, 40 μ m thick, were prepared and collected into the wells of 12-well tissue culture plates in cryoprotectant medium and stored at -20°C until immunostaining was performed. Two sections per mouse
5 were randomly selected for further study, based on full integrity of the sample, i.e., clearly delineated neocortex, and CA1, CA2 and CA3 were completely intact. Prior to immunohistochemistry, free-floating sections were placed individually in wells of 24-well tissue culture plates and
10 washed twice in phosphate-buffered saline (PBS; pH 7.4; containing calcium/magnesium). Sections were then permeabilized in PBS containing Triton X-100® (0.2%) for 20 min at room temperature. Sections were stained with antibodies to perform assessment of neuronal integrity.
15 Anti-synaptophysin IgG (Boehringer) was employed as a marker of presynaptic terminals. Anti-MAP-2 IgG (Boehringer) was employed as a marker of neuronal cell bodies/dendrites. The appropriate nonimmune IgG was employed as a control (Boehringer Mannheim). After appropriate blocking steps,
20 primary antibodies were incubated with sections and then washed in PBS. FITC-labeled secondary antibodies (Vector system; ABC) were employed to visualize sites of primary antibody binding. After washing, sections were mounted using Vectashield® on glass slides and then coverslips placed atop
25 the sections. Sections will then be kept in the dark at 4°C, for no more than two weeks prior to analysis.

Semiquantitative evaluation of neuronal integrity was performed using laser scanning confocal microscopy. Neuronal
30 integrity was assessed in the neocortex and pyramidal cell layer of the hippocampus (CA1 subfield) in six sections per mouse (two for each antibody marker). For each mouse, 4-8 confocal images (3-4/section) of the neocortex, and 2-4

confocal images (1-2/section) of the hippocampal CA1 subfield, each covering an area of 210 x 140 μm , were obtained. Under 60x, oil immersion, the sample was focused and iris and gain levels adjusted to obtain images with a pixel intensity within a linear range. Each final image was processed sequentially in Lasersharp. Digitized images were then transferred to a Macintosh computer using Adobe Photoshop, JPEG compression and analyzed with NIH Image. The area of the neuropil occupied by MAP-2-labeled dendrites or by synaptophysin-labeled presynaptic terminals was quantified and expressed as a percentage of the total image area as described²¹. Final analysis of digitized images for area neuropil occupied was determined by two independent investigators. Mean \pm standard deviation is reported for each section. Control sections were studied under conditions in which primary antibody was omitted, and no signal was observed with secondary antibody alone.

Immunostaining of mouse brain for other markers employed commercially available goat antibody to murine macrophage-colony stimulating factor (goat anti- M-CSF IgG; 10 $\mu\text{g}/\text{ml}$; Santa Cruz), rabbit antibody to activated caspase 3 (50 $\mu\text{g}/\text{ml}$; PharMingen), and mouse monoclonal antibody to phosphorylated tau (AT8; 10 $\mu\text{g}/\text{ml}$; Immunogenetics). In each case, the immunostaining protocol used standard techniques according to the manufacturer's instructions. Rabbit anti-murine Interleukin (IL) 6 IgG was provided by Dr. Gerald Fuller (University of Alabama Medical Center, Birmingham) and has been used in previous studies²². Sections were incubated with primary antibodies overnight at 4°C, followed by blocking with appropriate antisera and addition of biotin-conjugated goat anti-rabbit, goat anti-mouse or mouse anti-goat IgG (1:25 dilution) for 30 min at 37°C. Then ExtrAvidin

conjugated to peroxidase or to alkaline phosphatase (1:25 dilution) was added for 25 min at 37°C. Slides were then washed and developed with 3-amino-9-ethyl carbazole or fast red. Sections were viewed in an Olympus microscope, and 5 images were quantified using the Universal imaging system.

Activation of the transcription factor NF-kB was studied in brains of mice and in neurons cultured from this tissue (see below). Nuclear extracts were prepared according to the 10 method of Dignam et al.²³, and were incubated with ³²P-labelled double stranded consensus oligonucleotide probe for NF-kB (Santa Cruz) followed by polyacrylamide gel electrophoresis and autoradiography. These methods have been described previously using brain tissue and cultured cells 15 as the samples for preparation of nuclear extracts¹².

Isolation and characterization of neurons from Tg PD-ABAD mice. Brains of E16-18 mouse embryos were processed by a modification of a previously described method²⁴. In brief, 20 Embryos were washed in ethanol (75%), transferred to a dish with sterile phosphate-buffered saline (PBS) at 4°C under a tissue culture hood. Two embryos were dissected at a time immersed in Neurobasal Medium (GIBCO) with NaCl (22 mM), NaHCO₃ (4.4 mM), penicillin (50 units/ml) and streptomycin 25 (50 µg/ml). The embryo tail was removed and analyzed by PCR to determine genotype (as above). Cerebral cortex was dissected free from the cerebellum and brainstem, sliced into 1 mm pieces, and transferred to 1.5 ml eppendorf tubes in the above medium. The tube was centrifuged at 400 rpm, the 30 pellet was washed in PBS, and resuspended in PBS. Then, trypsin (0.25%; 0.5 ml) and DNase (250 units/ml) were added and the incubation was continued for 15 min at 37°C with gentle shaking. The mixture was decanted, washed twice in

PBS by inverting the tube and gently spinning at 400 rpm for 5 min. Neurons were cultured in growth medium (Neurobasal Medium with B27, 2%, L-glutamine, 2 mM, penicillin, 50 units/ml, streptomycin, 50 µg/ml) in wells coated with poly-L-lysine. Neurons were identified immunocytochemically using antibody to neurofilament (Sigma) and the methods for immunostaining described above.

¹³C-NMR spectroscopy. ¹³C NMR spectroscopy is a powerful technique for measuring substrate metabolism in tissue and cell culture²⁵⁻³¹. Addition to culture supernatant or perfusing organs with D-[2,4-¹³C]-3-hydroxybutyrate results in the [¹³C]-labelling of TCA cycle intermediates from labeled acetyl CoA^{29,30}. Although TCA cycle intermediates are usually present at concentrations too low to be observed by NMR spectroscopy, glutamate, which is present at millimolar concentrations, is in rapid exchange with α-ketoglutarate via aminotransferase reactions. Thus, if [¹³C]-labeled acetyl CoA enters the TCA cycle, the ¹³C-label will be detectable as [¹³C]-glutamate. For experiments with cultured cells (10⁷ cells/NMR determination), D-[¹³C]-β-hydroxybutyrate (10 mM) was added to DMEM (without glucose or pyruvate) and dialyzed fetal calf serum (10%). For in vivo studies, D-[¹³C]-β-hydroxybutyrate was infused intravenously as follows over 60 min: 0.75 M [¹³C]-β-hydroxybutyrate administered as a bolus (0.05 ml) followed by a constant infusion with a total volume of 1.5 ml³¹. At the end of the infusion, brain samples were freeze-clamped under liquid nitrogen and stored at -80°C. Frozen tissue (sample size, 92±6 and 88±11 mg, for Tg and nonTg mice, respectively) was extracted with perchloric acid, neutralized with sodium hydroxide as described²⁸⁻³⁰, and homogenates were lyophilized and resuspended in D₂O for NMR analysis. For cell culture studies, culture supernatants and

lysates were extracted with perchloric acid followed by neutralization and lyophilization as above.

High resolution carbon spectra were acquired on a Bruker 500
5 MHz spectrometer, using a 10 mm broad-band probe tuned to
125.77 MHz. Field homogeneity was optimized by shimming on
the D₂O lock signal. Spectra were obtained using a 25 KHz
sweep width, with 45° pulse and 2 s interpulse delay.
Heteronuclear decoupling was performed using a Waltz
10 sequence. Each spectrum represents a total of 17,920 scans.
The assignment of ¹³C resonances was based on previously
published studies^{26,27,29-31}. Glutamate peak areas were
determined using Bruker NMR software, and are expressed as
ratios with the summed area of the [2,4-¹³C]β-hydroxybutyrate
15 peaks. In brain extracts, the area measurements for
glutamate, glutamine and γ-amino butyric acid (GABA) are
compared with spectra obtained from an external standard
solution ([¹³C]-acetate, 0.1 M) using the same acquisition
parameters as above. The ¹³C NMR spectra of standard
20 solutions of glutamine and GABA were obtained to confirm
chemical shifts of these compounds in the brain extracts.

¹H NMR Spectroscopy. Water pre-saturation experiments were
acquired on the GE500 MHz spectrometer using a 5 mm inverse
25 detection probe (¹H observe, with broad band decoupling
capabilities). With a sweep width of 5 KHz, a 45° pulse
width, and the carrier frequency set on the H₂O peak for a 1
s pre-saturation pulse, ¹H spectra were obtained for 256
total scans. Presaturation experiments were performed both
30 with and without heteronuclear ¹³C decoupling (for assessing
the fractional enrichment in glutamate), centered at 40 ppm,
using a Waltz sequence.

The region between 2.6-2.0 ppm reveals proton resonances from the C-4 of glutamate. Although the proton resonances corresponding to [^{12}C -4]glutamate are resolvable, the ^1H satellites corresponding to [^{13}C -4]glutamate are obscured by other nearby peaks. Accordingly, the fractional enrichment of glutamate cannot be determined by measuring the areas of the proton peaks bound to labeled and nonlabeled carbons, as is the case with lactate²⁵. However, the enrichment of glutamate C-4 may be determined from the increase in intensity of the C-4 glutamate proton resonances following heteronuclear ^{13}C -decoupling, as these resolvable resonances then correspond to the sum of protons from labeled and nonlabeled glutamate²⁵.

Pa1 15 Induction of stroke in Tg PD-RAGE mice. Functional consequences of overexpression of RAGE were first assessed in response to ischemic stress, the transient middle cerebral artery occlusion model. *Murine stroke model* Mice (C57BL6/J, male) were subjected to stroke according to previously published procedures³². Following anesthesia, the carotid artery was accessed using the operative approach previously described in detail³³, including division/coagulation of the occipital and pterygopalatine arteries to obtain improved visualization and vascular access. A nylon suture was then introduced into the common carotid artery, and threaded up the internal carotid artery to occlude the origin of the right middle cerebral artery (MCA). Nylon (polyamide) suture material was obtained from United States Surgical Corporation (Norwalk, CT), and consisted of 5.0 nylon/13 mm length for 25 27-36 g mice, and 6.0 nylon/12 mm length for 22-26 g mice. After 45 minutes of occlusion, the suture was withdrawn to achieve a reperfused model of stroke. Although no vessels were tied off after the suture was removed, the external

carotid arterial stump was cauterized to prevent frank hemorrhage.

Measurements of *relative cerebral blood flow* were obtained as previously reported³²⁻³⁵ using a straight laser doppler flow probe placed 2 mm posterior to the bregma, and 6 mm to each side of midline using a stereotactic micromanipulator, keeping the angle of the probe perpendicular to the cortical surface. These cerebral blood flow measurements, expressed as the ratio of ipsilateral to contralateral blood flow, were obtained at baseline, and immediately prior to MCA occlusion, 45 minutes after MCA occlusion, and at several time points after withdrawal of the occluding suture.

Measurement of Cerebral Infarction Volumes: After 24 hours, animals were euthanized and their brains rapidly harvested. Infarct volumes were determined by staining serial cerebral sections with triphenyl tetrazolium chloride and performing computer-based planimetry of the negatively (infarcted) staining areas to calculate infarct volume (using NIH image software).

Neurological Exam: Prior to giving anesthesia, mice were examined for neurological deficit 23 h after reperfusion using a four-tiered grading system: a score of 1 was given if the animal demonstrated normal spontaneous movements; a score of 2 was given if the animal was noted to be turning towards the ipsilateral side; a score of 3 was given if the animal was observed to spin longitudinally (clockwise when viewed from the tail); and, a score of 4 was given if the animal was unresponsive to noxious stimuli. This scoring system has been previously described in mice³²⁻³⁴, and is based upon similar scoring systems used in rats³⁶. Immunostaining

of cerebral cortex following induction of stroke in wild-type mice was performed as described above using a rabbit polyclonal antibody made using purified recombinant murine ABAD as the immunogen. Quantitation of microscopic images was accomplished with the Universal Imaging System.

Results

Identification of Tg PD-ABAD mice. Southern analysis identifying three Tg PD-ABAD founders is shown in Fig. 2. These mice were used to generate lines of Tg PD-ABAD mice in whom the progeny were identified by PCR using the primers described in the methods section. An example of PCR detection of positive founders, versus negative non-Tg animals is shown in Fig. 3.

Characterization of Tg PD-ABAD mice. Expression of the transgene in the brain was determined by Northern analysis of total RNA extracted from cerebral cortex with ³²P-labelled cDNA for human ABAD (Fig. 4A). An intense band was observed in Tg PD-ABAD mice, but not in nontransgenic littermate controls. Similarly Western analysis was performed on protein extracts of cerebral cortex from transgenic mice using antibody to recombinant ABAD expressed in bacteria². Again, a strong band of immunoreactivity migrating just below the 30 kDa molecular weight marker confirmed the presence of high levels of ABAD antigen in brains of Tg PD-ABAD mice compared with nontransgenic littermate controls (Fig. 4B). Immunoblotting was then performed on brain subregions, including cerebral cortex, hippocampus and cerebellum, with anti-ABAD IgG (Fig. 5). In Tg PD-ABAD mice, intense immunoreactive bands were seen in cerebral cortex and hippocampus, compared with lower levels of transgene

expression in the cerebellum. Immunostaining with anti-ABAD IgG confirmed that the increased levels of ABAD in Tg PD-ABAD animals were in neurons (Fig. 4C-D). These data indicate that Tg PD-ABAD mice provide a model system in which neurons of the brain, especially cerebral cortex and hippocampus express high levels of ABAD.

NMR analysis of ^{13}C - β -hydroxybutyrate metabolism in Tg PD-ABAD mice. Tg PD-ABAD and control mice were infused with D-[2,4- ^{13}C]-3-hydroxybutyrate. ^{13}C NMR spectra of cerebral cortical extracts from Tg PD-ABAD and nonTg littermate control (the latter spectra are not shown) mice illustrate labelling of glutamate and glutamine in the C-4, C-3 and C-2 positions, as well as GABA (γ -aminobutyric acid) in the C-2 position (Fig. 6A), consistent with entry of [^{13}C]- β -hydroxybutyrate via 2-[^{13}C]-acetyl-CoA into the TCA cycle. The intensity of glutamate and glutamine C-4 resonance was 50% and 20% greater, respectively, in Tg PD-ABAD mice compared with nonTg littermates (Fig. 6B). The glutamate to glutamine ratio, based on C-4 resonance area, was 3.6 ± 0.3 in nonTg versus 2.1 ± 0.4 in Tg PD-ABAD mouse brains ($P < 0.03$). These data suggest that glutamine synthesis is more efficient in Tg PD-ABAD mouse brain compared with controls. The area of the ^{13}C -labelled C-2 resonance of GABA was also greater in Tg PD-ABAD mice (4.8 ± 0.3) than in nonTg controls (2.2 ± 0.5 ; $p < 0.04$). Such increased labelling of GABA is consistent with enhanced conversion of labelled glutamate to GABA in brains of Tg mice. ^1H NMR analysis of these extracts revealed that the fractional enrichment in glutamate C-4 was significantly greater in Tg PD-ABAD ($58 \pm 5\%$) than in nonTg littermates ($38 \pm 7\%$; $P < 0.03$). As might be expected from the increased utilization of exogenous β -hydroxybutyrate, measurement of basal ATP levels in cerebral cortex of Tg PD-ABAD mice fasted

overnight showed a statistically significant increase compared with nonTg littermates (Fig. 6C). Similarly, levels of β -hydroxybutyrate in the brains of Tg PD-ABAD mice were lower, compared with nonTg controls in view of its increased utilization in the presence of higher levels of neuronal ABAD (see Fig. 7D, animals not subjected to stroke). Thus, Tg PD-ABAD mice provide a means of detecting ABAD function because of their enhanced metabolism of exogenous β -hydroxybutyrate and their increased levels of ATP. These mice could provide a useful system for testing the effect of ABAD inhibitors on neurons in the context of an intact blood-brain barrier.

Induction of stroke in Tg PD-ABAD mice. In order to assess the possible contribution of ABAD to ischemic stress, Tg PD-ABAD and age-matched nonTg littermate control mice were subjected to a 45 min period of transient middle cerebral artery occlusion followed by a 24 hr period for evolution of the cerebral infarct. These studies utilized a protocol which we have found to provide reproducible stroke volumes and functional data (neurologic deficit scores, cerebral blood flow)³²⁻³⁵. Levels of ABAD increased an additional ≈ 2 -fold in Tg PD-ABAD mice after stroke, versus with uninstrumented Tg PD-ABAD mice. Compared with nonTg littermate controls, Tg PD-ABAD mice displayed strokes of smaller volume and lower neurologic deficit scores (consistent with better maintenance of neurologic function) (Fig. 7A-B). In contrast, there was no change in cerebral blood flow comparing the Tg and nonTg animals (not shown), consistent with a direct effect of ABAD on neurons, as ABAD was overexpressed in neurons by the PDGF B chain promoter. Analysis of cerebral cortex from Tg animals showed increased ATP and decreased lactate levels compared with nonTg controls (Fig. 7C). In addition, β -hydroxybutyrate

levels were lower in animals subjected to cerebral ischemia, and this finding was much more pronounced in Tg PD-ABAD mice compared with nonTg littermate controls (Fig. 7D). These data are suggested better maintenance of energy reserve and substrate metabolism in Tg PD-ABAD mice subject to ischemia.

Characterization of Tg PD-ABAD/hAPP mice. The increased expression of ABAD in AD brain, compared with age-matched non-demented control brain, suggested that the receptor might be associated with AD pathology. Consistent with this hypothesis, our pilot studies with Tg hAPP mice displayed increased levels of ABAD in cerebral cortex by 4 months of age, which is prior to plaque formation (not shown). Tg hAPP mice are especially useful for studies to assess the effect of introduction of the PD-ABAD transgene since they have been characterized in previous studies with respect to neuropathologic and electrophysiologic properties.

If ABAD exacerbated A β -induced neuronal stress, we reasoned that expression of high levels of ABAD at early times in the brains of animals expressing the hAPP transgene might result in magnified evidence of cytotoxicity (the transgenic model introduces higher levels of ABAD than were present in Tg hAPP mice alone, and thus, potentially represents a model of exaggerated effects of ABAD). Cross-breeding studies were performed and double transgenic mice were identified by PCR using primers specific for the PD-ABAD transgene and the hAPP transgene. Results of a representative PCR analysis are shown in Fig. 8 demonstrating amplicons for both the PD-ABAD and hAPP genes in the double-transgenic animals versus single transgenics and nontransgenic littermate controls. The double transgenic mice have been termed Tg PD-ABAD/hAPP mice.

Double transgenic mice were observed for three-four months and evidence of neuronal stress was then analyzed by studying expression of 4-hydroxynonenal (HNE; Fig. 9) and heme oxygenase type I (HO-1; Fig. 10). HNE-lysine epitopes were
5 determined by immunostaining with a monoclonal antibody followed by image analysis. Increased levels of HNE antigen were evident in the cerebral cortex of Tg PD-ABAD/hAPP by 4 months of age, compared with single transgenics and nontransgenic littermate controls (Fig. 9). Level of HO-1
10 were also increased in brains of double transgenic animals based on Northern analysis (Fig. 10A) and semiquantitative immunohistochemistry (Fig. 10B) in each case on samples of cerebral cortex.

15 These data were consistent with increased neuronal stress in Tg PD-ABAD/hAPP mice, but did not indicate whether the outcome of this stress would be neuroprotection or neurotoxicity. To analyze this situation neuropathologic studies were performed, and study of markers more clearly
20 associated with toxicity, such as synaptophysin and activated caspase 3, was undertaken. Immunostaining of hippocampus (lacunosum moleculare layer) from double transgenic mice (age 3-4 months) with antibody to synaptophysin demonstrated a reduction in the area of neuropil occupied by synaptophysin-
25 labeled presynaptic terminals, as well as the intensity of staining (Fig. 11). Similar studies with antibody to MAP-2 showed a reduction in the area of neuropil occupied by MAP-2-labeled dendrites (not shown). Although stereologic studies will be required to determine actual neuronal loss, these
30 results are consistent with evidence of neurotoxicity. Consistent with this impression, analysis of older double transgenic mice (8-9 months of age) showed increased staining with an antibody selective for the activated form of caspase

3 (Fig. 12) in brains of double transgenic mice compared with the other groups.

Characterization of neurons isolated from Tg PD-ABAD mice.

5 Neuronal cultures were made from the cerebral cortex from E16 mouse embryos. These cultures were >90% neurons based on staining with anti-neurofilament antibody (not shown). Cultured neurons displayed high levels of RAGE expression based on Northern analysis and immunoblotting (Fig. 13).

10

Discussion

We have described the generation of Tg PD-ABAD mice which
15 display increased expression of full-length ABAD in neurons. The use of these mice to analyze the contribution of ABAD to cellular responses *in vitro* and *in vivo* can be summarized according to three general categories:

20 1) analysis of neurons cultured from embryos of Tg PD-ABAD mice. Since neurons are nondividing cells and can only be transfected successfully with viral-based systems (which can alter cellular properties themselves), the cultured neurons from Tg PD-ABAD mice provide an unique system in
25 which neurons overexpress human ABAD. These cells can be used to analyze the consequences of ABAD expression in an A β -rich environment for neuronal function.

30 2) Tg PD-ABAD mice can be used to directly assess the effect of ABAD overexpression in settings such as, but not limited to, stroke (described above), viral/bacterial infections, other models of brain inflammation (such as experimental autoimmune encephalitis) etc.

3) Tg PD-ABAD mice can be crossbred with other transgenic animals, such as Tg hAPP to determine the consequences of ABAD overexpression in an environment in which the other transgene creates a unique environment in the brain. For example, the Tg hAPP mouse results in increased levels of A β . In this setting, the consequences of increased levels of A β in the context of neurons bearing elevated levels of ABAD can be studied.

10 In each case, the ~~in vitro and in vivo~~ systems based on Tg PD-ABAD mice or cells derived from them are ideal for studying RAGE inhibitors, as well as for dissecting contributions of ABAD to physiologic/pathophysiologic outcomes.

15

Example 2: Double Transgenic Mice Overexpressing ABAD and mutAPP (V717F, K670M, N671L) Show an Impairment of Hippocampal Long-Term Potentiation

20 Amyloid-beta peptide (A β) is the principal component of the extracellular deposits in Alzheimer's disease. However, means by which A β perturbs cellular functions are still unknown. It has been shown recently that A β binding alcohol dehydrogenase (ABAD), in an A β -rich environment is permuted
25 from a protective enzyme to a cofactor enhancing A β toxicity. In order to study the interaction of ABAD with mutAPP, double transgenic mice overexpressing both proteins in neurons under control of the PDGF-B chain promoter have been generated. Here, an investigation of basal synaptic transmission and
30 synaptic plasticity is shown in hippocampal slices from these animals. To measure basal synaptic transmission, we generated input-output curves by plotting the stimulus

voltage against the slope of the field EPSP. It was found that a 47% reduction in basal synaptic transmission in 10-month old mutAPP/ABAD mice (n=12) compared with wild type animals (n=11 slices, $P<0.001$). Transgenics overexpressing either mutAPP or ABAD alone did not show any change. Next, LTP was examined after a theta-burst stimulation in CA1 and observed that wild-type mice showed a 159% (n=10 slices) increase compared to baseline values 60 min after the stimulation, whereas mutAPP/ABAD littermates showed a 130% increase (n=9 slices, $P<0.05$). Single ABAD and mutAPP showed values comparable to wild-type animals. Thus, simultaneous overexpression of ABAD and mutAPP dramatically alters both basal synaptic transmission and synaptic plasticity.

15 Example 3: Enhanced Neuronal Stress and Cytotoxicity in Double Transgenic Mice With Targeted Overexpression of ABAD and Mutant Amyloid Precursor Protein (mutAPP)

Amyloid-beta peptide binding alcohol dehydrogenase (ABAD) is an intracellular enzyme capable of binding amyloid-beta peptide and promoting cell stress in vitro. To examine properties of ABAD in vivo, transgenic (Tg) mice overexpressing ABAD under control of the PDGF B chain promoter (Tg PD-ABAD) were made. These animals demonstrated increased ABAD antigen in neurons of cerebral cortex and hippocampus. Tg PD-ABAD mice were crossed with animals overexpressing a minigene encoding hAPP 695, 751 & 770 bearing mutations linked to familial Alzheimer's disease (Tg hAPP) to generate progeny which are double transgenics (Tg PC-ABAD/hAPP). By 4 months of age, Tg PD-ABAD/hAPP mice displayed increased neuronal stress, elevated 4-hydroxynonenal immunoreactivity (3-fold increased; $p<0.01$) and heme oxygenase type 1 (3-fold) were observed in cerebral

cortex of double transgenics compared with other groups. Semiquantitative immunohistochemistry for synaptophysin and microtubule-associated protein 2 showed decreases in both cases (25% and 25-30% respectively, compared with other groups; $p < 0.001$). Evidence of neurotoxicity was also suggested by increased levels of activated caspase 3 antigen in cortical neurons (3-4-fold increase compared with the other groups; $p < 0.001$). These data indicate that targeted neuronal overexpression of ABAD and hAPP exaggerates cell stress and promotes cytotoxicity.

Example 4: AMYLOID BETA-PEPTIDE BINDING ALCOHOL DEHYDROGENASE IS A COMPONENT OF THE CELLULAR RESPONSE TO NUTRITIONAL STRESS

Amyloid β -peptide Binding Alcohol Dehydrogenase (ABAD) is a member of the family of short-chain dehydrogenase/reductases whose distinctive properties include the capacity to bind amyloid beta-peptide ($A\beta$) and enzymatic activity towards a broad array of substrates including n-isopropanol and β -estradiol. In view of ABAD's wide substrate specificity and high activity on L- β -hydroxyacyl CoA derivatives, we asked whether it might also catalyze the oxidation of the ketone body D-3-hydroxybutyrate. This was indeed the case, and oxidation proceeded with K_m \sim 3.7 mM and V_{max} \sim 4 nmol/min/mg protein. When placed in medium with D- β -hydroxybutyrate as the principal energy substrate, COS cells stably transfected to overexpress wild-type ABAD (COS/wtABAD) better maintained 3-(4,5-dimethylthiazol-2-yl)-2,5-diphenyl tetrazolium bromide reduction, cellular energy charge and morphologic phenotype, compared with COS/vector cells. Using a severe model of metabolic perturbation, transgenic mice with targeted neuronal expression of ABAD subjected to transient middle

cerebral artery occlusion showed strokes of smaller volume and lower neurologic deficit scores in parallel with increased brain ATP and decreased lactate, compared with nontransgenic controls. These data suggest that ABAD
5 contributes to the protective response to metabolic stress, especially in the setting of ischemia.

INTRODUCTION

10 Recent studies of familial Alzheimer's disease have provided support for a close relationship between accumulation of amyloid beta-peptide ($A\beta$)¹, especially the longer form, $A\beta(1-42)$, and development of cerebral dysfunction leading to dementia (1-4). In sporadic Alzheimer's disease (AD), there
15 is an emerging view that decreased clearance of $A\beta$, possibly mediated by a pathway involving low density lipoprotein receptor-related protein, apoE and/or α_2 -macroglobulin, may contribute to the $A\beta$ -rich environment that disturbs cellular properties (5-8). However, much remains to be learned about
20 the pathways through which $A\beta$ actually induces cellular stress. In the presence of high concentrations of $A\beta$ (micromolar range), generation of oxidants and changes in calcium homeostasis feed into cell death pathways (9-12).

¹ Abbreviations: $A\beta$, amyloid- β peptide; AD, Alzheimer's disease; ABAD, $A\beta$ binding alcohol dehydrogenase; CoA, Coenzyme A; GABA, γ -amino butyric acid; MCA, middle cerebral artery; MTT, 3-(4,5-dimethylthiazol-2-yl)-2,5-diphenyl tetrazolium bromide; PD, platelet-derived growth factor B chain; SDR, short-chain dehydrogenase/reductase; TCA, tricarboxylic acid cycle; and, Tg, transgenic.

In order to understand mechanisms which might underlie A β -induced cell stress, rather than rapid induction of cell death, we have sought cell-associated cofactors capable of magnifying the effects of the amyloid peptide on target
5 cells. We reasoned that such cofactors might be relevant to early phases of AD when neuronal dysfunction is evolving, but changes are still reversible.

Amyloid β -peptide Binding Alcohol Dehydrogenase (ABAD) is a
10 member of the family of short-chain dehydrogenase/reductases (SDR) (13,14). It shares features with other members of this family, such as the requirement for a dinucleotide cofactor, nicotinamide adenine dinucleotide (NAD[H]), and a Rossmann-fold structural topology with an invariant sequence,
15 Tyr-X-X-X-Lys, corresponding to residues 168-172 in ABAD, all of which are required for enzymatic activity (15). However, it is distinct from other members of the family in terms of its ability to bind A β (13,14), and its ability to use a broad array of substrates, including linear alcohols,
20 3-hydroxyacyl-Coenzyme A (CoA) derivatives, and steroids (such as 17 β -estradiol) (13,14,16-19). In an A β -rich environment, ABAD appears to potentiate cell stress induced by the amyloid peptide, as evidenced by increased generation of 4-hydroxynonenal-lysine and malondialdehyde-lysine
25 epitopes and induction of DNA fragmentation (14). Although these observations suggest a "dark side" of ABAD potentially contributing to the pathogenicity of A β -induced cellular dysfunction, we reasoned that ABAD is likely to have other properties relevant to normal physiology. Consistent with
30 this concept, inactivation of the *Drosophila* counterpart of ABAD, termed *scully*, resulted in a lethal phenotype with multiple developmental abnormalities (20).

These broad enzymatic properties of ABAD suggested that it might facilitate utilization of ketone bodies, by promoting the generation of acetyl-CoA to feed into the tricarboxylic acid (TCA) cycle. This led us to consider a role for ABAD in the cellular response to nutritional/metabolic stress. For example, ketone bodies can reach appreciable concentrations (3-6 mM) in fasted nonhuman primates, both neonatal and infant animals (21), as well as during starvation in normal humans/adult animals (22-23). Under these conditions, the oxidation of β -hydroxybutyrate becomes the dominant source for energy production in brain (21-23). In the current study, we demonstrate that ABAD does promote utilization of ketone bodies in a cellular environment, probably at the level of both β -hydroxybutyrate. Furthermore, overexpression of ABAD in COS cells, which have low endogenous levels of this enzyme, maintains cellular functions under conditions where β -hydroxybutyrate is the principal energetic substrate. Using NMR to analyze [^{13}C]- β -hydroxybutyrate metabolism, ABAD-transfected COS cells displayed increased flux of acetyl-CoA through the TCA cycle. Since ischemia is a severe metabolic stress, a murine stroke model in transgenic mice was employed to determine consequences of overexpressing ABAD in cortical neurons. ABAD transgenic mice demonstrated a protective phenotype with ~40% reduction in stroke volume and improvement in neurologic deficit scores. Overexpression of ABAD in Tg mice was associated with increased flux of acetyl-CoA through the TCA cycle and increased ATP in cerebral cortex following infusion of β -hydroxybutyrate. These data indicate that expression of ABAD confers a protective phenotype in response to acute metabolic stress, such as that imposed by ischemia, and provide a starting point for further analysis of ABAD's properties in complex biologic systems.

MATERIALS AND METHODS

Recombinant ABAD and metabolism of β -hydroxybutyrate and β -hydroxybutyryl-CoA. ABAD was produced recombinantly in *E. Coli* (BL21) and purified to homogeneity as described (14). D- and L- β -hydroxybutyrate and D/L- β -hydroxybutyryl-CoA were obtained from Sigma. ABAD reduction of DL- β -hydroxybutyryl-CoA employed ABAD (330 ng/ml), a range of β -hydroxybutyryl-CoA concentrations (20-1000 μ M), and NAD⁺ (1.2 mM; Sigma) in Tris (75 mM; pH 10)/KCl (75 mM) (17). The reaction was run for a total of 10 min at 30°C under steady-state conditions (24), and the change in NADH absorbance at 340 nm was determined. ABAD reduction of either D- or L- β -hydroxybutyrate employed ABAD (150 μ g/ml), a range of β -hydroxybutyrate concentrations (0.4-25 mM), and NADH (5 mM) in Tris (10 mM; pH 7.4)/NaCl (25 mM). β -hydroxybutyrate, NADH and Tris/NaCl were preincubated for 10 min at 37°C. Then, the enzyme was added, and the reaction was run for a total of 30 min at 30°C under steady-state conditions as above, except that absorbance at 340 nm was determined every 5 min. Kinetic data were analyzed for Michaelis-Menton by PRISM (Scitech, San Diego, CA) to determine K_m and V_{max} , and lines shown in the figures represent theoretical curves according to kinetic parameters calculated by the program. One unit of enzyme activity was defined as that which converts 1.0 μ mol of substrate to product per min. All studies to determine kinetic parameters of ABAD were performed 3-5 times.

30

Generation and characterization of stably-transfected COS cells expressing ABAD. COS cells (ATCC; 10^5 cells) were transfected with pcDNA3/(human) wild-type ABAD or mutABAD,

or pcDNA3 alone (vector) previously linearized with SmaI, using lipofectamine (14). MutABAD, in which residues 168 (Y) and 172 (K) in the active site have been replaced by glycine, generating an enzymatically crippled enzyme, has been previously characterized (14). Forty-eight hours after transfection, cells were plated at 1:10-1:20 dilution in 100 mm dishes containing G418 (1 mg/ml), and, after 1-2 wks, single clones were isolated, cells were separated with trypsin, subject to limiting dilution and replated in medium containing G418 (1 mg/ml) for 2-4 wks. Cultures were then maintained in DMEM with fetal bovine serum (Gibco, Grand Island, NY; 10%) and G418 (1 mg/ml), and ABAD expression was characterized as described below. For Northern blotting, total RNA was isolated using Trizol (Gibco) and run on 1% agarose gels, transferred to nitrocellulose, and hybridized with a full length ³²P-labelled cDNA probe for ABAD (13,14).

For immunoblotting, cell lysates, prepared by directly lysing cell pellets in SDS sample buffer, were subjected to SDS-PAGE (reduced; 12%) followed by transfer to nitrocellulose. The Blotto procedure was used (25); the first antibody was anti-ABAD peptide IgG (10 µg/ml), and the second antibody was peroxidase-conjugated goat anti-rabbit IgG (1:2000 dilution; Sigma, St. Louis MO) in the ECL secondary antibody/detection system (Amersham, Arlington Hts, IL). Anti-ABAD peptide IgG was prepared and characterized as described previously (13,14).

Subcellular fractionation of ABAD employed ultracentrifugation of cells disrupted by nitrogen cavitation bomb, as described (14). Following disruption, the lysate was clarified by centrifugation at 10,000 x g for 15 min at 4°C, and the pellet was resuspended in buffer containing tris/HCl (10 mM; pH 8.0)/Nonidet P-40 (1%), NaCl (150 mM),

EDTA (1 mM), aprotonin (1 μ g/ml), and phenylmethanesulfonyl fluoride (1 mM). This material was centrifuged and fractionated through a series of sucrose steps (38, 30, and 20% sucrose prepared in HEPES [10 mM; pH 7.5]/dithiothreitol [1 mM]). Layered fractions were collected as described (28), and each fraction (5 μ g protein/lane) was analyzed by immunoblotting with anti-ABAD peptide IgG. The following markers of subcellular compartments were employed: RAGE for cell membranes (anti-RAGE IgG was prepared as described) (26,27), GRP78/Bip for endoplasmic reticulum (antibody to GRP78/Bip was obtained from StressGen[®], Victoria, Canada) (28), and cytochrome c for mitochondria (antibody to cytochrome c was obtained from StressGen[®]). The mitochondria-rich fraction was also prepared as described by Du et al. (29).

¹³C-NMR spectroscopy. ¹³C NMR spectroscopy is a powerful technique for measuring substrate metabolism in tissue and cell culture (30-38). Addition to culture supernatant or perfusing organs with D-[2,4-¹³C]-3-hydroxybutyrate results in the [¹³C]-labelling of TCA cycle intermediates from labeled acetyl CoA (36,37). Although TCA cycle intermediates are usually present at concentrations too low to be observed by NMR spectroscopy, glutamate, which is present at millimolar concentrations, is in rapid exchange with α -ketoglutarate via aminotransferase reactions. Thus, if [¹³C]-labeled acetyl CoA enters the TCA cycle, the ¹³C-label will be detectable as [¹³C]-glutamate. For experiments with cultured cells (10⁷ cells/NMR determination), D-[¹³C]- β -hydroxybutyrate (10 mM) was added to DMEM (without glucose or pyruvate) and dialyzed fetal calf serum (10%). For *in vivo* studies, D-[¹³C]- β -hydroxybutyrate was infused intravenously as follows over 60 min: 0.75 M

[¹³C]-β-hydroxybutyrate administered as a bolus (0.05 ml) followed by a constant infusion with a total volume of 1.5 ml (38). At the end of the infusion, brain samples were freeze-clamped under liquid nitrogen and stored at -80°C.

5 Frozen tissue (sample size, 92±6 and 88±11 mg, for Tg and nonTg mice, respectively) was extracted with perchloric acid, neutralized with sodium hydroxide as described (35-37), and homogenates were lyophilized and resuspended in D₂O for NMR analysis. For cell culture studies, culture supernatants and

10 lysates were extracted with perchloric acid followed by neutralization and lyophilization as above.

High resolution carbon spectra were acquired on a Bruker 500 MHz spectrometer, using a 10 mm broad-band probe tuned to

15 125.77 MHz. Field homogeneity was optimized by shimming on the D₂O lock signal. Spectra were obtained using a 25 KHz sweep width, with 45° pulse and 2 s interpulse delay. Heteronuclear decoupling was performed using a Waltz sequence. Each spectrum represents a total of 17,920 scans.

20 The assignment of ¹³C resonances was based on previously published studies (33,34,36-38). Glutamate peak areas were determined using Bruker NMR software, and are expressed as ratios with the summed area of the [2,4-¹³C]β-hydroxybutyrate peaks. In brain extracts, the area measurements for

25 glutamate, glutamine and γ-amino butyric acid (GABA) are compared with spectra obtained from an external standard solution ([¹³C]-acetate, 0.1 M) using the same acquisition parameters as above. The ¹³C NMR spectra of standard solutions of glutamine and GABA were obtained to confirm

30 chemical shifts of these compounds in the brain extracts.

¹H NMR Spectroscopy. Water pre-saturation experiments were acquired on the GE500 MHz spectrometer using a 5 mm inverse

detection probe (^1H observe, with broad band decoupling capabilities). With a sweep width of 5 KHz, a 45° pulse width, and the carrier frequency set on the H_2O peak for a 1 s pre-saturation pulse, ^1H spectra were obtained for 256 total scans. Presaturation experiments were performed both with and without heteronuclear ^{13}C decoupling (for assessing the fractional enrichment in glutamate), centered at 40 ppm, using a Waltz sequence.

10 The region between 2.6-2.0 ppm reveals proton resonances from the C-4 of glutamate. Although the proton resonances corresponding to [^{12}C -4]glutamate are resolvable, the ^1H satellites corresponding to [^{13}C -4]glutamate are obscured by other nearby peaks. Accordingly, the fractional enrichment
15 of glutamate cannot be determined by measuring the areas of the proton peaks bound to labeled and nonlabeled carbons, as is the case with lactate (32). However, the enrichment of glutamate C-4 may be determined from the increase in intensity of the C-4 glutamate proton resonances following
20 heteronuclear ^{13}C -decoupling, as these resolvable resonances then correspond to the sum of protons from labeled and nonlabeled glutamate (32).

Assays of Cellular Function: MTT reduction and measurement
25 of cellular energy charge. Reduction of 3-(4,5-dimethylthiazol-2-yl)-2,5-diphenyl tetrazolium bromide (MTT) was studied and phase contrast micrographs of COS cells were made as previously described (13,39). Measurement of cellular energy charge was also performed by previous methods
30 (40). In brief, cultured cells previously incubated in D- β -hydroxybutyrate, DMEM without glucose or sodium pyruvate (Gibco/BRL), and dialyzed fetal calf serum (10%; Gibco/BRL) were washed three times in phosphate-buffered saline.

Adenine nucleotides were extracted with perchloric acid (1 M), and subjected to centrifugation through a layer of bromododecane. The supernatant was neutralized with potassium hydroxide and subjected to reversed-phase HPLC
5 (Microsorb C18; Rainin Instruments Co., Woburn, MA). The column eluate was monitored at an absorbance of 254 nm, and nucleotide concentration was calculated from the peak area using ChromatoPack CR-4A (Shimadzu Seiki, Kyoto, Japan). At each point the energy charge was calculated as described
10 (41).

Generation and characterization of ABAD transgenic mice. The platelet-derived growth factor (PDGF) B-chain promoter was used to drive overexpression of ABAD in neurons of the
15 central nervous system of transgenic (Tg) mice (42). Transgene constructs were prepared using a previously described vector (43,44). Briefly, the CMV immediate/early promoter was excised from the commercial expression vector pCI (Promega, Madison WI), and replaced with an
20 oligonucleotide polylinker. The PDGF B-chain promoter fragment was mobilized as an XbaI fragment (42) and cloned into a unique SpeI site designed within the synthetic linker. The full-length human ABAD cDNA was inserted into the NotI site of the original polylinker. A 3 kb fragment containing
25 the promoter, cDNA and required other sequences was then excised from the plasmid backbone as BamHI fragment and microinjected into mouse B6CBAF₁/J oocytes. The latter were implanted into pseudopregnant females and mated with B6CBAF₁/J males resulting in the generation of four founders.
30 These were used to produce lines, which were backcrossed eight times into the C57BL6 background. Tg PD-ABAD mice were identified by Southern blotting, and expression of the transgene was monitored by Northern and Western blotting, and

immunostaining. Southern blotting was performed on DNA extracted from mouse tails, and hybridization was performed with ³²P-labelled cDNA probe for ABAD. Northern and immunoblotting utilized the same procedures as above, except
5 that tissue was homogenized in the presence of Trizol (RNA) or in lysis buffer (Tris/HCl, 20 mM, pH 7.4; Triton X-100, 1%; phenylmethanesulfonylfluoride, 2 mM; EDTA, 1 mM; aprotonin, 10 µg/ml; leupeptin, 10 µg/ml; 1 ml of buffer per 0.5 gm of tissue). Note that immunoblotting and
10 immunostaining of brain tissue from Tg PD-ABAD mice used anti-human ABAD peptide IgG which appears to be preferentially immunoreactive with human ABAD, the latter encoded by the transgene (13). Immunostaining was performed on paraformaldehyde (4%)-embedded sections (6 µm) which were
15 deparaffinized and dehydrated, and then stained with rabbit anti-human ABAD peptide IgG (8.5 µg/ml) followed by goat anti-rabbit biotin-conjugated IgG and ExtrAvidin-conjugated with alkaline phosphatase (Biotin ExtrAvidin kit; Sigma, St. Louis MO).

20
Murine stroke model. Mice (C57BL6/J, male) were subjected to stroke according to previously published procedures (45) and in accordance with guidelines of the American Academy of Accreditation of Laboratory Animal Care (AAALAC). Following
25 anesthesia, the carotid artery was accessed using the operative approach previously described in detail (46), including division/coagulation of the occipital and pterygopalatine arteries to obtain improved visualization and vascular access. A nylon suture was then introduced into the
30 common carotid artery, and threaded up the internal carotid artery to occlude the origin of the right middle cerebral artery (MCA). Nylon (polyamide) suture material was obtained from United States Surgical Corporation (Norwalk, CT), and

consisted of 5.0 nylon/13 mm length for 27-36 g mice, and 6.0 nylon/12 mm length for 22-26 g mice. After 45 minutes of occlusion, the suture was withdrawn to achieve a reperfused model of stroke. Although no vessels were tied off after the suture was removed, the external carotid arterial stump was cauterized to prevent frank hemorrhage. Measurements of relative cerebral blood flow were obtained as previously reported (45-48) using a straight laser doppler flow probe placed 2 mm posterior to the bregma, and 6 mm to each side of midline using a stereotactic micromanipulator, keeping the angle of the probe perpendicular to the cortical surface. These cerebral blood flow measurements, expressed as the ratio of ipsilateral to contralateral blood flow, were obtained at baseline, and immediately prior to MCA occlusion, 45 minutes after MCA occlusion, and at several time points after withdrawal of the occluding suture. Measurement of Cerebral Infarction Volumes: After 24 hours, animals were euthanized and their brains rapidly harvested. Infarct volumes were determined by staining serial cerebral sections with triphenyl tetrazolium chloride and performing computer-based planimetry of the negatively (infarcted) staining areas to calculate infarct volume (using NIH image software). Neurological Exam: Prior to giving anesthesia, mice were examined for neurological deficit 23 h after reperfusion using a four-tiered grading system: a score of 1 was given if the animal demonstrated normal spontaneous movements; a score of 2 was given if the animal was noted to be turning towards the ipsilateral side; a score of 3 was given if the animal was observed to spin longitudinally (clockwise when viewed from the tail); and, a score of 4 was given if the animal was unresponsive to noxious stimuli. This scoring system has been previously described in mice (45-47), and is based upon similar scoring

systems used in rats (49). Immunostaining of cerebral cortex following induction of stroke in wild-type mice was performed as described above using a rabbit polyclonal antibody made using purified recombinant murine ABAD as the immunogen.

5 Quantitation of microscopic images was accomplished with the Universal Imaging System

ATP and lactate/pyruvate ratio were determined in cerebral cortex from control mice, and from ischemic versus

10 nonischemic hemispheres of mice subjected to ischemia (measurements were made 24 hrs after induction of ischemia). Perchloric acid-extracted cerebral cortex was neutralized with sodium hydroxide and the ATP in the extract was measured using HPLC techniques (50). Lactate, β -hydroxybutyrate and

15 pyruvate levels in the neutralized extracts were measured using established assays (51).

RESULTS

20 ABAD metabolism of β -hydroxybutyrate. The broad enzymatic properties of ABAD as an oxidoreductase suggested that it might facilitate cellular utilization of ketone bodies, such as D- β -hydroxybutyrate, a major energetic substrate during nutritional deprivation *in vivo*. First, we tested

25 DL- β -hydroxybutyryl-CoA, a known substrate of bovine liver-derived hydroxyacyl-CoA type II (HADH II)/ABAD (17), with our purified *E. Coli*-derived human recombinant ABAD; the reaction fit Michaelis-Menton kinetics with K_m was 134 μ M and V_{max} 26.3 μ mol/min/mg (Fig. 1A). The latter result,

30 obtained with a racemic DL mixture of β -hydroxybutyryl CoA, was similar to that observed previously with the bovine liver HADH II (17). Using the same preparation of recombinant ABAD, we then studied D- β -hydroxybutyrate; the reaction also

fit best to Michaelis-Menton kinetics with K_m was ~ 3.7 mM, and V_{max} was ~ 4 nmol/min/mg (Fig. 1B). With the L-form of β -hydroxybutyrate, K_m was ~ 1.6 mM, and V_{max} ~ 3.5 nmol/min/mg (Fig. 1C). In a purified system, ABAD is clearly more effective with β -hydroxybutyryl-CoA as a substrate (presumably this is the L-form, which is an intermediate in the fatty acid β -oxidation pathway in mitochondria). However, depending on physiological conditions, certain substrates may turn out to be more abundant, such as D- β -hydroxybutyrate during periods of starvation when levels of ketone bodies are elevated and, thus, could become relevant. In fact, plasma levels of β -hydroxybutyrate are reported to reach the millimolar range in animals and humans subject to nutritional deprivation (21-23). Furthermore, β -hydroxybutyryl CoA generated by acyl CoA dehydrogenase is another likely substrate of ABAD in a cellular milieu rich in β -hydroxybutyrate. Thus, ABAD would appear to have the potential to be pivotal for enhancing metabolism of β -hydroxybutyrate.

Characterization of COS cells stably-transfected to overexpress ABAD. COS cells provided a useful model to test our concept that ABAD modulated the cellular response to nutritional stress because of their low endogenous expression of ABAD; low levels of mRNA were present (Fig. 2A, lane 4) and no antigen was detectable (Fig. 2B, lane 7) in lysates of wild-type COS cells. Following stable transfection with either pcDNA3 alone (vector), pcDNA3/wtABAD (encoding wild-type ABAD) or pcDNA3/mutABAD (encoding a mutant form of ABAD devoid of enzymatic activity; 14), cells were plated at limiting dilution and clones were prepared. Three types of clones were established, those expressing vector alone (COS/vector), wild-type ABAD (COS/wtABAD) and mutant ABAD

(COS/mutABAD). Studies were performed with three representative clones of each type of stably-transfected COS cell. Whereas COS/vector cells displayed low levels of ABAD transcripts (Fig. 2A, lanes 3) and antigen (Fig. 2B, lanes 6), comparable to control COS cells, COS/wtABAD cells showed high levels of ABAD mRNA (Fig. 2A, lanes 2) and antigen (Fig. 2B, lanes 3-5). Subcellular fractionation studies on COS/wtABAD cells (Fig. 2C, line a) demonstrated the presence of ABAD both in fractions 1-2 enriched for the endoplasmic reticulum marker GRP78 (Fig. 2C, line c) and in the mitochondrial pellet (fraction 6) containing cytochrome c (Fig. 2C, line e). Similar experiments performed with COS/mutABAD stable transfectants (Fig. 2C, line b) displayed high levels of ABAD transcripts (Fig. 2A, lane 1) and antigen (Fig. 2B, lanes 1-2) in a distribution analogous to that seen in COS/wtABAD cells. These data indicated that in COS/ABAD stable transfectants, the enzyme is present at the same sites previously observed in cells endogenously expressing ABAD or those transiently transfected to overexpress ABAD (13,14,16,19).

ABAD and the response of COS cells to nutritional stress.
In view of ABAD metabolism of D- β -hydroxybutyrate, we tested whether ABAD-transfected COS cells displayed enhanced ability to sustain nutritional stress in an environment where ketone bodies provided the principal energetic source. When COS/vector cells were placed in medium devoid of glucose and supplemented only with dialyzed serum and β -hydroxybutyrate, cellular functions became compromised. In the presence of D- β -hydroxybutyrate (10 mM), reduction of MTT was suppressed by days 4-5 (Fig. 3A) and cellular energy charge decreased in parallel (Fig. 3C). Phase contrast microscopy showed COS/vector cells, initially with a spread morphology on the

growth substrate, to become rounded up and toxic in appearance after four days under these conditions (Fig. 3DI-II). Similar results were obtained when COS/vector cells were replaced with wild-type COS cells, and the same studies described above were performed (not shown). In contrast, COS/wtABAD cells better maintained MTT reduction (Fig. 3A) and cellular energy charge (Fig. 3C) in the presence of β -hydroxybutyrate. These changes in cellular properties were paralleled by maintenance of the morphologic phenotype of COS/wtABAD cells, compared with COS/vector transfectants (Fig. 3DIII-IV) in the presence of β -hydroxybutyrate. The effect of β -hydroxybutyrate to maintain cellular functions in COS/wtABAD cells was dose-dependent, as shown using the MTT reduction assay, and reached a plateau by 10 mM (Fig. 3B). Furthermore, experiments with lower concentrations of β -hydroxybutyrate (2.5 mM) displayed less effective maintenance of cellular properties with COS/wtABAD cells (not shown). The requirement for enzymatically intact ABAD (wtABAD) for enhanced survival of COS/wtABAD cells in the presence of β -hydroxybutyrate was shown by experiments performed with COS/mutABAD cells. Though the crippled enzyme (mutABAD) was expressed at similar levels and with a similar subcellular distribution as the wild-type enzyme (the latter in COS/wtABAD cells), COS/mutABAD cells responded to glucose replacement with β -hydroxybutyrate as did COS/vector cells; there was a steady decline in MTT reduction and cellular energy charge (Fig. 3A,C).

NMR studies were performed on cells incubated with [^{13}C]-D- β -hydroxybutyrate (labelled in the C-2 and C-4 positions) to determine the effect of ABAD on the metabolism of the COS/wtABAD transfectants in medium devoid of glucose. [^{13}C]-labelled β -hydroxybutyrate enters the TCA cycle as

[¹³C-2]-labelled acetyl-CoA and is metabolized to α-ketoglutarate. Thus, C-4 gets labelled in the first turn of the TCA cycle, and, subsequent, labelling occurs in the C-3 and C-2 positions. As α-ketoglutarate is in rapid equilibrium with glutamate, the labelling of [¹³C]-glutamate in the C-4, 3 and 2 positions was observed (Fig. 4A). Since the flux of [¹³C]labelled acetyl-CoA via the TCA cycle is orientation conserved, the labelling of [¹³C]-glutamate is greater in the C-4, compared with the C-3 and C-2, positions. Thus, labelling was evaluated in the C-4 position of glutamate in COS/wtABAD versus COS/vector in cell lysates and supernatants. In culture supernatants, NMR data demonstrated greater labelling of the C-4 resonances in glutamate in COS/wtABAD cells, 2-fold, compared with COS/vector cells (Fig. 4B; p<0.03 at days 4, 6 and 8). Glutamine was not detected in supernatants from COS/wtABAD or COS/vector cells. The ¹H NMR analysis of these supernatants revealed that the fractional enrichment at glutamate C-4 was 58±3% in COS/wtABAD transfectants compared with 41±2% in COS/vector cells. These data are indicative of increased metabolism of exogenous [¹³C]-labelled β-hydroxybutyrate in COS cells overexpressing ABAD. In contrast, there were no observed differences between fractional enrichment at glutamate C-4 in cell lysates between COS/wtABAD and COS/vector cells, probably because glutamate is rapidly extruded into the medium (glutamine and glutamate levels in cell lysates were the same, comparing COS/wtABAD and COS/vector cells). The ¹³C and ¹H NMR data demonstrate increased exogenous β-hydroxybutyrate utilization in the COS cells overexpressing wtABAD.

Upregulation of ABAD in response to cerebral ischemia. A severe form of metabolic stress is imposed by cerebral

ischemia. Wild-type C57BL6 mice subjected to transient middle cerebral artery occlusion displayed increased levels of ABAD in neurons near the infarcted area (Fig. 5A), especially those in the penumbra (Fig. 5A, inset), compared with the nonischemic hemisphere (Fig. 5B), using polyclonal antibody to recombinant mouse ABAD. Image analysis of multiple fields from sections similar to those shown in panels A-B demonstrated an ~5-fold increase of ABAD antigen in cortical neurons consequent to stroke (Fig. 5C).

10

Characterization of Tg PD-ABAD mice. These data with wild-type mice subjected to cerebral ischemia suggested that upregulation of ABAD might be a component of the response to ischemic stress, and led us to make transgenic mice in which ABAD was overexpressed in cortical neurons. Three independent founders of Tg mice in which human ABAD is expressed under control of the human PDGF B-chain promoter have been identified and used to establish transgenic lines (at present backcrossed eight times into the C57BL6 background). Representative mice from each of these transgenic lines showed high levels of transgene activity at both the mRNA (Fig. 6A) and protein levels (Fig. 6B) in cerebral cortex. Immunoblotting performed on brain subregions from one line of Tg PD-ABAD mice, using an anti-human ABAD peptide antibody which selectively recognizes the human form of the protein, showed increased antigen especially in cerebral cortex and hippocampus, with a smaller increase in cerebellum (Fig. 6C). Immunohistochemical staining of ABAD in cerebral cortex confirmed high levels of antigen expression in cortical neurons (Fig. 6D1) compared with nontransgenic littermates (Fig. 6D2). Semiquantitative analysis of immunohistochemical results using antibody reactive with murine and human ABAD antigen (i.e., total ABAD

25

30

antigen) indicated that there was an 3.5-4-fold increase in total ABAD antigen in cerebral cortex comparing Tg mice with nonTg littermate control mice (Fig. 6D3). Induction of stroke in transgenic mice further elevated ABAD antigen another two-fold compared with nonTg controls (24 hrs after the ischemic episode; not shown). Growth (height/weight) and reproductive fitness (number and size of litters) was similar between Tg PD-ABAD mice and nontransgenic (nonTg) controls, and there were no overt neurologic symptoms or other phenotype evident in these mice noted to date.

NMR analysis of ^{13}C - β -hydroxybutyrate metabolism in Tg PD-ABAD mice. Tg PD-ABAD and control mice were infused with D-[2,4- ^{13}C]-3-hydroxybutyrate. ^{13}C NMR spectra of cerebral cortical extracts from Tg PD-ABAD and nonTg littermate control (the latter spectra are not shown) mice illustrate labelling of glutamate and glutamine in the C-4, C-3 and C-2 positions, as well as GABA in the C-2 position (Fig. 7A), consistent with entry of [^{13}C]- β -hydroxybutyrate via 2-[^{13}C]-acetyl-CoA into the TCA cycle. The intensity of glutamate and glutamine C-4 resonance was 50% and 20% greater, respectively, in Tg PD-ABAD mice compared with nonTg littermates (Fig. 7B). The glutamate to glutamine ratio, based on C-4 resonance area, was 3.6 ± 0.3 in nonTg versus 2.1 ± 0.4 in Tg PD-ABAD mouse brains ($P < 0.03$). These data suggest that glutamine synthesis is more efficient in Tg PD-ABAD mouse brain compared with controls. The area of the ^{13}C -labelled C-2 resonance of GABA was also greater in Tg PD-ABAD mice (4.8 ± 0.3) than in nonTg controls (2.2 ± 0.5 ; $p < 0.04$). Such increased labelling of GABA is consistent with enhanced conversion of labelled glutamate to GABA in brains of Tg mice. ^1H NMR analysis of these extracts revealed that the fractional enrichment in glutamate C-4 was significantly

greater in Tg PD-ABAD ($58 \pm 5\%$) than in nonTg littermates ($38 \pm 7\%$; $P < 0.03$). As might be expected from the increased utilization of exogenous β -hydroxybutyrate, measurement of basal ATP levels in cerebral cortex of Tg PD-ABAD mice fasted overnight showed a statistically significant increase compared with nonTg littermates (Fig. 7C). Similarly, levels of β -hydroxybutyrate in the brains of Tg PD-ABAD mice were lower, compared with nonTg controls in view of its increased utilization in the presence of higher levels of neuronal ABAD (see Fig. 8D, animals not subjected to stroke).

Induction of stroke in Tg PD-ABAD mice. In order to assess the possible contribution of ABAD to ischemic stress, Tg PD-ABAD and age-matched nonTg littermate control mice were subjected to a 45 min period of transient middle cerebral artery occlusion followed by a 24 hr period for evolution of the cerebral infarct. These studies utilized a protocol which we have found to provide reproducible stroke volumes and functional data (neurologic deficit scores, cerebral blood flow) (45-48). Levels of ABAD increased an additional 2-fold in Tg PD-ABAD mice after stroke, versus with uninstrumented Tg PD-ABAD mice. Compared with nonTg littermate controls, Tg PD-ABAD mice displayed strokes of smaller volume and lower neurologic deficit scores (consistent with better maintenance of neurologic function) (Fig. 8A-B). In contrast, there was no change in cerebral blood flow comparing the Tg and nonTg animals (not shown), consistent with a direct effect of ABAD on neurons, as ABAD was overexpressed in neurons by the PDGF B chain promoter. Analysis of cerebral cortex from Tg animals showed increased ATP and decreased lactate levels compared with nonTg controls (Fig. 8C). In addition, β -hydroxybutyrate levels were lower in animals subjected to cerebral ischemia,

and this finding was much more pronounced in Tg PD-ABAD mice compared with nonTg littermate controls (Fig. 8D). These data are suggested better maintenance of energy reserve and substrate metabolism in Tg PD-ABAD mice subject to ischemia.

5

DISCUSSION

ABAD is a member of the short-chain dehydrogenase/reductase family with remarkably broad substrate specificity, now
10 extended to include the ketone body D- β -hydroxybutyrate. In comparison with mitochondrial D- β -hydroxybutyrate dehydrogenase (52-55), which displays K_m \sim 1 mM, ABAD is similar with K_m \sim 3.7 mM. At β -hydroxybutyrate concentrations in the plasma of normal individuals (<1 mM), both enzymes
15 would be working considerably below their respective K_m 's. Under pathologic conditions, when β -hydroxybutyrate concentrations can reach the millimolar range (21-23), both enzymes would be expected to metabolize β -hydroxybutyrate. However, the maximal activity of ABAD (0.0037 μ mole/min/mg)
20 is much lower than that for the mitochondrial enzyme, V_{max} \sim 100-175 μ moles/min/mg protein with β -hydroxybutyrate (54,55). D- β -hydroxybutyrate dehydrogenase is a housekeeping metabolic enzyme present in mitochondria whose expression has not been reported to vary in pathologic states, beyond its
25 loss from severely ischemic cardiac tissue (56-57). ABAD, present in both endoplasmic reticulum and mitochondria, displays a pattern of expression sensitive to environmental perturbations, including increased expression in brains of patient's with Alzheimer's disease (13) and at sites of
30 ischemic brain injury. Thus, in settings where ABAD expression is enhanced, the enzyme could, potentially, contribute to the metabolism of β -hydroxybutyrate. However, the situation is likely to be more complex *in vivo*, since Tg

PD-ABAD mice display increased flux of acetyl-CoA through the TCA cycle and higher ATP levels in the cerebral cortex, even though the level of ABAD expression is only increased by about 3.5-4-fold, compared with nontransgenic controls.

5 These data indicate that ABAD clearly has the potential to contribute to β -hydroxybutyrate metabolism, though the extent of its contribution is likely to depend on the particular situation.

hall 10 Increased expression of ABAD in human brain following cerebral infarction² and in response to experimentally-induced cerebral ischemia (Fig. 5) suggests that induction of ABAD might subserve normal protective mechanisms. In view of the complexities of cellular
15 metabolic pathways, it was necessary to prove that ABAD could promote metabolic homeostasis in response to nutritional deprivation. ABAD-transfected COS cells displayed increased energy charge and flux of acetyl-CoA through the TCA cycle in medium containing β -hydroxybutyrate compared with controls
20 in which the active site of ABAD was mutationally inactivated. Enhanced metabolic homeostasis was reflected by maintenance of MTT reduction and morphologic phenotype in ABAD-transfected COS cells. Similarly, transgenic mice overexpressing ABAD in cortical neurons demonstrated
25 increased flux of acetyl-CoA through the TCA cycle following β -hydroxybutyrate infusion compared with nontransgenic littermates. However, increased basal levels of ATP (and energy charge; data not shown) in brains of Tg PD-ABAD mice, even before nutritional stress, was unexpected, and suggests

² Unpublished observation, Yan, S-D., and Stern, D., 1999.

a more general protective potential of ABAD in response to a range of environmental challenges. This apparent increase in the overall energy charge in the presence of ABAD, implies that the enzyme may render neurons metabolically more stable
5 and, thus, less susceptible to fluctuations in substrate availability.

A decreased lactate content in the cerebral cortex of Tg PD-ABAD mice subjected to stroke suggests two important
10 events associated with neuroprotection. First, decreased tissue lactate and lower lactate/pyruvate ratio in the Tg PD-ABAD mice are indicative of diminished cytosolic NADH/NAD⁺ ratio and consistent with decreased reductive stress. In this context, studies have suggested that diminished in
15 reductive stress may translate into lower reactive oxygen species generation upon reperfusion (58). Second, decreased tissue lactate is also indicative of efficient lactate efflux in stroke-prone tissue thereby alleviating feedback inhibition brought about by metabolic intermediates of
20 glycolysis (59-61).

Our NMR measurements were based on conversion of α -ketoglutarate, an intermediate in the TCA cycle, to glutamate. However, we also observed conversion of
25 glutamate, thus formed, to glutamine and GABA. These data indicate that ketone bodies, such as β -hydroxybutyrate, can provide both a substrate for maintenance for cellular energy charge, as well as a source for increased production of neurotransmitters. To our knowledge, this is the first time
30 that the conversion of labelled β -hydroxybutyrate to GABA and glutamate has been demonstrated *in vivo*. Furthermore, the increased production of ¹³C-labelled GABA and glutamate from [¹³C]- β -hydroxybutyrate in Tg PD-ABAD mice, compared with

controls, indicates that ABAD provides a novel means for sustaining energy production and replenishing neurotransmitters in the brain using ketone bodies as the substrate. At this point, it is unclear whether
5 neuroprotection afforded by overexpression of ABAD is due solely to its effect on ATP levels and/or changes in neurotransmitter metabolism.

In contrast to this cytoprotective facet of ABAD biology, we
10 have proposed that in the presence of A β , another, quite different, aspect of ABAD's properties becomes manifest (14). In an A β -rich environment, ABAD generates reactive oxygen intermediates and toxic reactive aldehydes based on cotransfection experiments using cultured COS and
15 neuroblastoma cells(14)(unpublished observation)². Furthermore, pilot studies with double transgenic mice, resulting from a cross of Tg PD-ABAD mice with transgenic mice overexpressing mutant β APP, have shown accelerated expression of cell stress markers (4-hydroxynonenal and heme
20 oxygenase type 1), compared with single transgenic mice, and nontransgenic controls². Based on these data, ABAD appears to have chameleon-like properties depending on the local environment, in particular related to the presence of A β . Our future studies have the goal of determining how ABAD's
25 properties become modulated in an A β -rich environment, and whether this translates into accelerated and more severe neuronal dysfunction/toxicity. The current studies provide a foundation for evaluating metabolic properties of ABAD in response to cellular stress *in vitro* and *in vivo*.

30

~~REFERENCES~~

1. Hardy, J. (1997) *TrendsNeurosci.* **20**, 28570-26998
2. Citron, M., Westaway, D., Xia, W., Carlson, G., Diehl,

- T., Levesque, G., Johnson-Wood, K., Lee, M., Seubert, P., Davis, A., Kholodenko, D., Motter, R., Sherrington, R., Perry, B., Yao, H., Strome, R., Lieberburg, I., Rommens, J., Kim, S., Schenk, D., Fraser, P., St. George-Hyslop, P., and Selkoe, D. (1997) *NatureMed.* **3**, 67-72
3. St. George-Hyslop, P (1998) *Neurobiol. Aging* **19**, 133-137
4. Selkoe, D. (1999) *Ann. Rev. Cell Biol.* **10**, 373-403
5. Liao, A., Nitsch, R., Greenberg, S., Finckh, U., Blacker, D., Albert, M., Rebeck, G., Gomez-Isla, T., Clatworthy, A., Binetti, G., Hock, C., Mueller-Thomsen, T., Mann, U., Zuchowski, K., Beisiegel, U., Staehelin, H., Growdon, J., Tanzi, R., and Hyman, B. (1998) *Human Molec. Gen.* **12**, 1953-1956
6. Kisilevsky, R., Lemieux, J., Fraser, P., Kong, X., Hultin, P., and Szarek, W. (1995) *Nature Med.* **1**, 143-148
7. Goldgaber, D., Schwarzman, A., Bhasin, R., Gregori, L., Schmechel, D., Saunders, A. M., Roses, A. D., and Strittmatter, W. J. (1993) *Annals New York Acad. Sci.* **695**, 139-143
8. Roses, A. (1998) *Ann. New York Acad. Sci.* **855**, 738-743
9. Hensley, K., Carney, J., Mattson, M., Aksenova, M., Harris, M., Wu, J., Floyd, R., and Butterfield, D. (1994) *Proc. Natl. Acad. Sci. (U. S. A.)* **91**, 3270-3274
10. Mattson, M. and Goodman, Y. (1995) *Brain Res.* **676**, 219-224
11. Mark, R., Blanc, E., and Mattson, M. (1996) *Mol. Neurobiol.* **12**, 915-924
12. Mattson, M. (1995) *Neurobiol. Aging* **16**, 679-682
13. Yan, S. D., Fu, J., Soto, C., Chen, X., Zhu, H., Al-Mohanna, F., Collison, K., Zhu, A., Stern, E., Saido, T., Tohyama, M., Ogawa, S., Roher, A., and

- Stern, D. (1997) *Nature(Lond.)* **389**, 689-695
14. Yan, S-D., Shi, Y., Zhu, A., Fu, J., Zhu, H., Zhu, Y.,
Gibson, L., Collison, K., Al-Mohanna, F., Ogawa, S.,
Roher, A., Clarke, S., and Stern, D. M. (1998) *J. Biol.*
5 *Chem.* **274**, 2145-2156
15. Jornvall, H., Persson, B., Krook, M., Atrian, S.,
Duarte-Gonzalez, R., Jeffer, J., and Ghosh, D. (1995)
Biochemistry **34**, 6003-6013
16. Furuta, S., Kobayashi, A., Miyazawa, S., and Hashimoto,
10 T. (1997) *Biochim. Biophys. Acta.* **1350**, 317-324
17. Kobayashi, A., Jiang, L., and Hashimoto, T. (1996) *J.*
Biochem. **119**, 775-782
18. He, X-Y., Schulz, H., and Yang, S-Y. (1998) *J. Biol.*
Chem. **273**, 10741-10746
- 15 19. He, X-Y., Merz, G. , Mehta, P., Schulz, H., and Yang,
S-Y. (1999) *J. Biol. Chem.* **274**, 15014-15019
20. Torroja, L., Ortuno-Sahagun, D., Ferrus, A., Hammerle,
B., and Barbas, J. (1998) *J. Cell. Biol.* **141**, 1009-1017
21. Levitsky, L., Fisher, D., Paton, J., and Delannoy, C.
20 (1977) *Pediatr. Res.* **11**, 298-302
22. Owen, O., Morgan, A., Kemp, H., Sullivan, J., Herrera,
M., and Cahill. G. (1967) *J. Clin. Invest.* **46**,
1589-1595
23. Petersson, B., Settergren, G., and Dahlquist, G. (1972)
25 *Acta Paediat. Scand.* **61**, 273-277
24. Segel, I. H. (1975) *Enzyme Kinetics, Behavior, and*
Analysis of Rapid Equilibrium and Steady-State Enzyme
Systems, Wiley-Interscience, New York
25. Johnson, D., Gautsch, J., Sportsman, J., and Elder, J.
30 (1984) *Gene Anal. Tech.* **1**, 3-8
26. Schmidt, A. M., Vianna, M., Gerlach, M., Brett, J.,
Ryan, J., Kao, J., Esposito, C., Hegarty, H., Hurley,
W., Clauss, M., Wang, F., Pan, Y. C., Tsang, T. C., and

- Stern, D. M. (1992) *J. Biol. Chem.* **267**, 14987-14997
27. Schmidt, A. M., Hori, O., Brett, J., Yan, S. D.,
Wautier, J. L., and Stern, D. M. (1994) *Arterioscler.
Thromb.* **14**, 1521-1528
- 5 28. Kuwabara, K., Matsumoto, M., Ikeda, J., Ogawa, S.,
Maeda, Y., Kitagawa, K., Imuta, N., Kinoshita, T.,
Stern, D., Yangi, H., and Kamada, T. (1996) *J. Biol.
Chem.* **271**, 5025-5032
29. Du, Y., Dodel, R., Bales, K., Jemmerson, R.,
10 Hamilton-Byrd, E., and Paul, S. (1997) *J. Neurochem.*
69, 1382-1388
30. Sonnewald, U., Westergaard, N. Hassel, B., Muller, T.,
Unsgard, G., Fonnum, F., Hertz, L., Schousboe, A., and
Petersen, S. (1993) *Dev. Neurosci.* **15**, 351-358
- 15 31. Badar-Goffer, R., Bachelard, H., and Morris, P. (1990)
Biochem. J. **266**, 133-139
32. Jones, J., Hansen, J., Sherry, A., Malloy, C., and
Victor, R. (1997) *Analytical Biochemistry* **249**, 201-206
33. London, R. (1988) *Prog. NMR Spectroscopy* **20**, 337-383
- 20 34. Malloy, C., Sherry, A., and Jeffrey, F. (1987) *FEBS
Lett.* **212**, 58-62
35. Trueblood, N. and Ramasamy, R. (1998) *Am. J. Physiol.*
275, H75-H83
36. Chatham, J., Forder, J., Glickson, J., and Chance, E.
25 (1995) *J. Biol. Chem.* **270**, 7999-8008
37. Jeffrey, F., Diczku, V., Sherry, A., and Malloy, C.
(1995) *Basic Res. Cardiol.* **90**, 388-396
38. Fitzpatrick, S., Hetherington, H., Behar, K., and
Shulman, R. (1990) *J. Cereb. Blood Flow and Metab.* **10**,
30 170-179
39. Behl, C., Davis, J., Lesley, R., and Schubert, D.
(1994) *Cell* **77**, 817-827
40. Imuta, N., Ogawa, S., Maeda, Y., Kuwabara, K., Hori,

- O., Ueda, H., Tanagihara, T., and Tohyama, M. (1998) *J. Neurochem.* **70**, 550-557
41. Ueda, H., Hashimoto, T., Furuya, E., Tagawa, K.,
Kitagawa, K., Matsumoto, M., Yoneda, S., Kimura, K.,
5 and Kamada, T. (1988) *J. Biochem. (Tokyo)* **104**, 81-86
42. Sasahara, M., Fries, J., Raines, E., Gown, A., Westrum,
L., Frosch, M., Bonthron, D., Ross, R., and Collins, T.
(1991) *Cell* **64**, 217-227
43. Kang, D., Soriano, S., Frosch, M., Collins, T., Naruse,
10 S., Sisodia, S., and Koo, E. (1999) *J. Neurosci.* **19**,
4229-4237
44. Berezovska, O., Frosch, M., McLean, P. Knowles, R.,
Koo, E., Kang, D., Lu, F., Lux, S., Shen, J., Onegawa,
S., Hyman, B., (1999) *Brain Res. Mol. Brain Res.* **69**,
15 273-280
45. Huang, J., Kim, L., Mealey, R., March, H., Zhang, A.,
Tenner, E., Connolly, E., and Pinsky, D. (1999) *Science*
285, 595-599
46. Connolly, E. S., Winfree, C. J., Stern, D. M., Solomon,
20 R. A., and Pinsky, D. J. (1996) *Neurosurg.* **38**, 523-532
47. Connolly, E., Winfree, C., Springer, T., Naka, Y.,
Liao, H., Yan, S-D., Stern, D., Solomon, R.,
Gutierrez-Ramos, J-C., and Pinsky, D. (1996) *J. Clin.*
Invest. **97**, 209-216
- 25 48. Connolly, E., Winfree, C., Prestigiacomo, C., Kim, S.,
Choudhri, T., Hoh, B., Naka, Y., Solomon, R., and
Pinsky, D. (1997) *Circ. Res.* **81**, 304-310
49. Bederson, J. B., Pitts, L. H., and Tsuji, M. (1986)
Stroke **17**, 472-476
- 30 50. Sellevold, O., Jynge, P., and Aarstad, K. (1986) *J.*
Mol. Cell. Cardiol. **18**, 517-527
51. Lamprecht, W. and Heinz, F. (1995) *Method of Enzymatic*
Analysis, Verlag Chemie, Boca Raton, FL

52. McCann, W. (1957) *J. Biol. Chem.* **226**, 15-22
53. Lehninger, A., Sudduth, H., and Wise, J. (1960) *J. Biol. Chem.* **235**, 2450-2455
54. Bock, H., and Fleischer, S. (1975) *J. Biol. Chem.* **250**,
5 5774-5781
55. McIntyre, J., Latruffe, N., Brenner, S., and Fleischer, S. (1988) *Arch. Biochem. Biophys.* **262**, 85-98
56. Evertsen, F., Medbo, J., Jebens, E., and Gjovaag, T. (1999) *Acta Physiol. Scand* **167**, 247-257
- 10 57. Frederiks, W., Tukkier, R., Grundeman, P., Schellens, J. (1995) *J. Pathol.* **175**, 339-348
58. Williamson, J., Chang, K., Frangos, M., Hasan, K., Ido, Y., Kawamura, T., Nyengaard, J., Van den Enden, M., Kilo, C., and Tilton, R. (1993) *Diabetes* **42**, 801-813
- 15 59. Neely, J. and Morgan, H. (1974) *Ann. Rev. Physiol.* **36**, 413-459
60. King, L. and Opie, L. (1998) *Mol. Cell. Biochem.* **180**, 3-26
61. Lipton, P. (1999) *Physiol. Rev.* **79**, 1431-1568

20

The following description of figures are provided as descriptions of the results from Example 4. There are no pictures/illustrations/drawings submitted to correspond to these descriptions.

25

FIGURE LEGENDS

Figure 1. ABAD metabolism of β -hydroxybutyrate and β -hydroxybutyryl-CoA. A. ABAD (330 ng/ml) was incubated with the indicated concentration of D/L- β -hydroxybutyryl-CoA and NAD⁺ (1.2 mM). B-C. ABAD (200 μ g/ml) was incubated with the indicated concentration of D- β -hydroxybutyrate (B) or L- β -hydroxybutyrate (C) and NAD⁺ (5 mM). The velocity (V) of the reaction (units/mg of protein) is plotted versus added

30

substrate concentration. Details of experimental methods are described in the text. The line represents the theoretical curve according to the K_m and V_{max} values calculated by the computer program.

5

Figure 2. Characterization of COS cells stably-transfected to overexpress ABAD. A. RNA isolated from stably-transfected COS cells, either COS/mutABAD (lane 1), COS/wtABAD (lane 2) or COS/vector (lane 3), or wild-type COS
10 cells (lane 4) was subjected to Northern analysis (30 μ g of total RNA was added to each lane). Membranes were hybridized with 32 P-labelled cDNA probe for ABAD, and RNA loading was determined based on the intensity of the 18S ribosomal RNA band on ethidium bromide-stained gels. B. Protein extracts
15 from stably-transfected COS cells (COS/mutABAD, lanes 1-2; COS/wtABAD, lanes 3-5; and, COS/vector, lane 6) or wild-type COS cells (lane 7) were subjected to SDS-PAGE (12%; reduced; 100 μ g of total protein was added to each lane) followed by immunoblotting with anti-ABAD IgG (10 μ g/ml). In each case
20 (lanes 1-2 and 3-5), protein extracts were obtained from different clones of stable transfectants. The migration of simultaneously run molecular weight standards is shown on the far right side of the gel. C. Stably-transfected COS cells (COS/wtABAD, line a, and COS/mutABAD, line b) were subjected
25 to subcellular fractionation by nitrogen bomb cavitation followed by ultracentrifugation through a series of sucrose steps, and collection of fractions (1-6). Immunoblotting was performed on fractions using anti-ABAD IgG (a-b), anti-GRP78 IgG (c; as a marker of endoplasmic reticulum), anti-RAGE IgG
30 (d; as a marker of plasma membrane), and anti-cytochrome c IgG (e; as a marker of mitochondria).

Figure 3. Properties of COS/ABAD stable transfectants:

effect of D- β -hydroxybutyrate-containing medium. A. COS/wtABAD, COS/mutABAD and COS/vector stable transfectants were placed in DMEM (without glucose or pyruvate) containing D- β -hydroxybutyrate (10 mM) and dialyzed fetal calf serum (10%). MTT reduction was measured on the indicated day. B. The experiment was performed with stably-transfected COS cells as in A for five days at the indicated concentration of D- β -hydroxybutyrate. C. The experiment was performed with stably-transfected COS cells as in A with medium containing D- β -hydroxybutyrate (10 mM). On the indicated day, energy charge (E.C.) was determined. D. COS/ABAD and COS/vector cells maintained in the above medium containing D- β -hydroxybutyrate (10 mM) as above were photographed on day 0 (just after placement in the medium; panels I&III) or 4 days after incubation under these conditions (panels II&IV). Experiments were repeated a minimum of three times.

Figure 4. The effect of ABAD overexpression on the proton-decoupled ^{13}C NMR spectrum of supernatant from cells perfused with D-[2,4- ^{13}C] β -hydroxybutyrate. A. The spectrum from COS/vector (top panel) and COS/ABAD (bottom panel) cells in DMEM (without glucose or pyruvate) containing D- ^{13}C - β -hydroxybutyrate (10 mM) and dialyzed fetal calf serum (10%) displays prominent glutamate peaks. Abbreviations: G-2, G-3, G-4 denote the position 2, 3 and 4 carbons of glutamate, respectively; B-2 and B-4 denote carbon 2 and 4 of β -hydroxybutyrate. B. The effect of ABAD overexpression on the area of glutamate C-4 resonance in the supernatant from studies as in A. Values are expressed as the ratio of the areas of the C-4 peak over the summed areas of β -hydroxybutyrate peaks. * indicates glutamate areas were significantly higher in COS/ABAD than COS/vector cells ($P < 0.03$). The areas are reported as mean \pm standard

deviation.

Figure 5. Immunohistologic analysis of ABAD in murine cerebral ischemia. Mice were subjected to the transient middle cerebral artery occlusion model, allowed to recover for 24 hr, and then sacrificed. Immunohistologic analysis of formalin-fixed, paraffin-embedded sections of cerebral cortex was performed with rabbit anti-mouse ABAD IgG (20 μ g/ml). Panel **A** shows a low power view (marker bar= 10 μ m) of the infarcted area (* denotes the center of the infarcted area) displaying sites of ABAD expression, and the inset shows the penumbral region. Note the presence of ABAD in neurons. Panel **B** shows the nonischemic hemisphere. Panel **C** shows the results of image analysis of 5 fields similar to those shown in A-B analyzed using the Universal Imaging System. *indicates $p < 0.0001$.

Figure 6. Characterization of Tg PD-ABAD mice. **A.** Northern analysis for ABAD transcripts in cerebral cortex from mice representing three different lines of Tg PD-ABAD animals (lanes 1-3) and three non-transgenic littermate controls (lanes 4-6). Cerebral cortex was harvested from 3-4 month old mice, total RNA was prepared, subjected to electrophoresis on agarose (5%) gels (30 μ g of RNA was added to each lane) followed by transfer to membranes and hybridization with 32 P-labelled ABAD cDNA (RNA loading was estimated by ethidium bromide staining of the 28S ribosomal RNA band). **B.** Western analysis was performed on protein extracts from cerebral cortex of mice representing three lines of Tg PD-ABAD animals (lanes 1,2&6) and from three nontransgenic littermate controls (lanes 3-5). Cerebral cortex was harvested from 3-4 month old mice, protein extracts were prepared and subjected to SDS-PAGE (12%;

reduced; 100 μ g of protein was added to each lane)/immunoblotting with anti-ABAD IgG (10 μ g/ml). C. Immunoblotting was performed on the indicated brain subregion of one Tg PD-ABAD mouse using anti-human ABAD peptide IgG with 100 μ g of total protein extract loaded in each case (this antibody does not react with endogenous ABAD murine epitopes). Representative results are shown with a mouse from one line of Tg PD-ABAD mice, and these experiments were repeated three times with different mice from the same line of Tg PD-ABAD animals. D. Immunohistochemical study of cerebral cortex from the brain of a Tg PD-ABAD mouse (D1) with anti-human ABAD peptide IgG (10 μ g/ml) displaying the presence of the antigen in cortical neurons compared with a nonTg control mouse (D2). D3. Semiquantitative analysis of immunohistochemical results in Tg PD-ABAD and nonTg littermate controls as described in the text.

Figure 7. The effect of ABAD overexpression on the proton-decoupled ^{13}C NMR spectra of freeze-clamped brain after perfusion with D-[2,4- ^{13}C] β -hydroxybutyrate. A. The spectrum from a representative Tg PD-ABAD mouse displays prominent glutamate and glutamine peaks. The inset shows expanded regions of resonances of glutamate (G-4), glutamine (GL-4) and GABA (GA-2) from Tg (PD-ABAD) mice. Abbreviations: G-2, G-3, and G-4 denote the position 2, 3, and 4 carbons of glutamate, respectively; GL-2, GL-3 and GL-4 denote the position 2, 3 and 4 carbons of glutamine, respectively; and, GA-2 corresponds to C-2 of GABA. B. The effect of ABAD overexpression on areas of glutamate C-4 resonance in brain extracts of Tg PD-ABAD and nonTg littermate control mice as obtained from ^{13}C - NMR analysis. Values are expressed as the ratio of the area of the glutamate C-4 peak over the area of an added standard acetate

(see Methods). *Glutamate and glutamine levels were significantly higher in Tg PD-ABAD mice than in nonTg controls ($P < 0.03$; $N = 4$, in each case). Total areas of ^{13}C -glutamate (G-2 + G-3 + G-4) were significantly higher in the Tg PD-ABAD compared with nonTG littermate controls. C. Basal ATP- levels in whole brain extracts from Tg PD-ABAD ($N = 5$) or nonTg littermate controls ($N = 5$) were measured as described in the text. Animals were fasted overnight, and the brain was removed and freeze-clamped for ATP and β -hydroxybutyrate (BHB) analysis. * indicates $P < 0.03$. In each case, the data is reported as the mean \pm SD.

Figure 8. Induction of stroke in Tg PD-ABAD mice. A-B. Tg PD-ABAD mice and nonTg littermates were subjected to middle cerebral artery occlusion and were evaluated 24 hrs after the ischemic insult to determine neurologic deficit score (B), and, following sacrifice, infarct volume (A). C-D. At the same time point, cerebral cortex was harvested to determine ATP, lactate and β -hydroxybutyrate (BHB) levels determined on extracts of whole brains (from animals subjected to the stroke procedure 24 hrs previously) from Tg PD-ABAD or nonTg control mice ($N = 5$, in each case). Data is reported as the mean \pm SD ($P < 0.04$ for ATP and $P < 0.03$ for lactate).

25 Summary

Amyloid β -peptide Binding Alcohol Dehydrogenase (ABAD) is a member of the family of short-chain dehydrogenase/reductases whose distinctive properties include the capacity to bind amyloid beta-peptide ($\text{A}\beta$) and enzymatic activity towards a broad array of substrates. In view of ABAD's properties as a 3-hydroxyacyl-CoA dehydrogenase, the hypothesis was tested that this enzyme would promote the cellular response to

nutritional deprivation when ketone bodies are important energetic substrates. This hypothesis has proven to be correct based on experimental evidence from *in vitro* and *in vivo* studies presented in this manuscript. Stably-transfected
5 COS cells overexpressing ABAD incubated in with medium devoid of glucose, and supplemented with β -hydroxybutyrate and dialyzed serum displayed enhanced metabolic homeostasis compared with vector-transfected COS cells (maintenance of energy charge, MTT reduction and morphologic phenotype). In
10 addition, we have made transgenic mice overexpressing ABAD under control of the platelet-derived growth factor B chain promoter (Tg PD-ABAD) which are shown to have high levels of ABAD in cortical neurons. Consistent with our *in vitro* results, transient middle cerebral artery occlusion (a severe
15 model of nutritional deprivation) in Tg PD-ABAD mice resulted in strokes of smaller volume and lower neurologic deficit scores compared with nontransgenic littermate controls. Tg mice also showed increased flux of acetyl-CoA through the TCA cycle, as well as increased labelling of glycogen and
20 elevated ATP levels in cerebral cortex compared with nontransgenic controls. These data suggest that ABAD contributes to the protective response to metabolic stress, especially in the setting of ischemia.

Q13
References

1. Yan SD, Fu J, Soto C, Chen X, Zhu H, Al-Mohanna F, Collison K, Zhu A, Stern E, Saido T, Tohyama M, Ogawa S, Roher A, Stern D: An intracellular protein that bind amyloid-beta peptide and mediates neurotoxicity in Alzheimer's disease. *Nature(Lond)* 1997;389:689-695
2. Yan S-D, Shi Y, Zhu A, Fu J, Zhu H, Zhu Y, Gibson L, Collison K, Al-Mohanna F, Ogawa S, Roher A, Clarke S, Stern DM: Role of ERAB/L-3-hydroxyacyl-Coenzyme A dehydrogenase type II activity in amyloid beta-peptide-induced cytotoxicity. *J Biol Chem* 1998;274:2145-2156
3. Furuta S, Kobayashi A, Miyazawa S, Hashimoto T: Cloning and expression of cDNA for a newly identified iszyme of bovine liver 3-hydroxyacyl-CoA dehydrogenase and its import into mitochondria. *Biochim Biophys Acta* 1997;1350:317-324
4. Kobayashi A, Jiang L, Hashimoto T: Two mitochondrial 3-hydroxyacyl-CoA dehydrogenases in bovine liver. *J Biochem* 1996;119:775-782
5. He X-Y, Schulz H, Yang S-Y: A human brain L-3-hydroxyacyl-coenzyme A dehydrogenase is identical to amyloid beta-peptide-binding protein involved in Alzheimer's disease. *J Biol Chem* 1998;273:10741-10746
6. He X-Y, Merz G, Mehta P, Schulz H, Yang S-Y: Human brain short chain L-3-hydroxyacyl Coenzyme A dehydrogenase is a single-domain multifunctional enzyme. *J Biol Chem* 1999;274:15014-15019

7. Torroja L, Ortuno-Sahagun D, Ferrus A, Hammerle B, Barbas J: scully, an essential gene of Drosophila, is homologous to mammalian mitochondrial type II L-3-hydroxyacyl-CoA dehydrogenase/Amyloid-beta peptide-binding protein. *J Cell Biol* 1998;141:1009-1017
8. Sasahara M, Fries J, Raines E, Gown A, Westrum L, Frosch M, Bonthron D, Ross R, Collins T: PDGF B-chain in neurons of the central nervous system, posterior pituitary and in a transgenic model. *Cell* 1991;64:217-227
9. Kang D, Saitoh T, Chen X, Xia Y, Maslian E, Hansen L, Thomas R, Thal L, Katzman R: Genetic association of LRP with late-onset Alzheimer's disease. *Neurology* 1997;49:56-61
10. Berezovska O, Frosch M, McLean P, Knowles R, Koo E, Kang D, Shen J, Lu F, Lux S, Tonegawa S, Hyman B: The Alzheimer-related gene presenilin 1 facilitates notch 1 in primary mammalian neurons. *Molec Brain Res* 1999;69:273-280
11. Laemmli U: Cleavage of structural proteins during the assembly of the head of bacteriophage T4. *Nature* 1970;227:680-685
12. Yan S-D, Chen X, Chen M, Zhu H, Roher A, Slattery T, Zhao L, Nagashima M, Morser J, Migheli A, Nawroth P, Stern DM, Schmidt A-M: RAGE and amyloid-beta peptide neurotoxicity in Alzheimer's disease. *Nature* 1996;382:685-691
13. Yan S-D, Zhu H, Zhu A, Golabek A, Roher A, Yu J, Soto C, Schmidt A-M, Stern DM, Kindy M: Receptor-dependent cell stress and amyloid accumulation in systemic amyloidosis. *Nat Med* 2000;6:643-651

14. Hsia A, Masliah E, McConlogue L, Yu G-Q, Tatsuno G, Hu
K, Kholodenko D, Malenka R, Nicoll R, Mucke L:
Plaque-independent disruption of neural circuits in
Alzheimer's disease mouse models. *Proc Natl Acad Sci (USA)*
5 1999;96:3228-3233
15. Terry R, Masliah E, Salmon D, Butters N, DeTeresa R, Hill
R, Hansen L, Katzman R: Physical basis of cognitive
alterations in Alzheimer disease: synapse loss is the major
10 correlate of cognitive impairment. *Ann Neurol* 1991;30:572-580
16. Zhan S, Beyreuther K, Schmitt H: Quantitative assessment
of synaptophysin immunoreactivity of the corticla neuropil
in various neurodegenerative diseases with dementia. *Dementia*
15 1993;4:66-74
17. Dickson D, Crystal H, Bevona C, Honer W, Vincent I,
Davies P: Correlation of synaptic and pathological markers
incognition in the elderly. *Neurobiol Aging* 1995;16:285-304
20
18. Sze C, Troncoso J, Kowas C, Mouton P, Price D, Martin J:
Loss of presynaptic vesicle protein synaptophysin in
hippocampus correlates with cognitive decline in Alzheimer
disease. *J Neuropathol Exp Neurol* 1997;56:933-944
25
19. Samuel W, Alford M, Hofstetter C, Hansen L: Dementia with
Lewy bodies versus pure Alzheimer disease: differences in
cognition, neuropathology, cholinergic dysfunction, and
synapse density. *J Neuropathol Exp Neurol* 1997;56:499-508
30
20. Brown D, Risser R, Bigio E, Tripp P, Stiegler A, Welch
E, Eagan K, Hladik C, White C: Neocortical synatpic density
and Braak stage in Lewy body variant of Alzheimer disease.

J Neuropathol Exp Neurol 1998;58:955-960

21. Masliah E, Achim C, Ge N, DeTeresa R, Terry R, Wiley C:
The spectrum of human immunodeficiency virus-associated
5 neocortical damage. *Ann Neurol* 1992;32:321-329
22. Yan S-F, Tritto I, Pinsky DJ, Liao H, May L, Stern DM:
Induction of interleukin 6 (IL-6) by hypoxia in vascular
cells: central role of the binding site for nuclear
10 factor-IL-6. *J Biol Chem* 1995;270:11463-11471
23. Dignam J, Lebovitz R, Roeder R: Accurate transcription
initiation by RNA polymerase II in a soluble extract from
isolated mammalian nuclei. *Nucl Acids Res* 1983;11:1475-1489
15
24. White A, Zheng H, Galatis D, Maher F, Hesse L, Multhaup
G, Beyreuther K, Masters C, Cappai R: Survival of cultured
neurons from amyloid precursor protein knock-out mice against
Alzheimer's amyloid- β toxicity and oxidative stress. *J*
20 *Neurosci* 1998;18:6207-6217
25. Jones J, Hansen J, Sherry A, Malloy C, Victor R:
Determination of acetyl-CoA enrichment in rat heart and
skeletal muscle by ^1H nuclear magnetic resonance analysis of
25 glutamate in tissue extracts. *Analytical Biochemistry*
1997;249:201-206
26. London R: ^{13}C labelling in studies of metabolic
regulation. *Prog NMR Spectroscopy* 1988;20:337-383
30
27. Malloy C, Sherry A, Jeffrey F: Carbon flux through citric
acid cycle pathways in perfused heart by ^{13}C NMR
spectroscopy. *FEBS Lett* 1987;212:58-62

28. Trueblood N, Ramasamy R: Aldose reductase inhibition improves altered glucose metabolism of isolated diabetic rat hearts. *Am J Physiol* 1998;275:H75-H83
- 5 29. Chatham J, Forder J, Glickson J, Chance E: Calculation of absolute metabolic flux and the elucidation of the pathways of glutamate labelling in perfused rat heart by ¹³C NMR spectroscopy and nonlinear least squares analysis. *J Biol Chem* 1995;270:7999-8008
- 10 30. Jeffrey F, Diczku V, Sherry A, Malloy C: Substrate selection in the isolated working rat heart: effects of reperfusion, afterload, and concentration. *Basic Res Cardiol* 1995;90:388-396
- 15 31. Fitzpatrick S, Hetherington H, Behar K, Shulman R: Flux from glucose to glutamate in the rat brain in vivo as determined by ¹H-observed, ¹³C-edited NMR spectroscopy. *J Cereb Blood Flow and Metab* 1990;10:170-179
- 20 32. Huang J, Kim L, Mealey R, March H, Zhang A, Tenner E, Connolly E, Pinsky D: Neuronal protection in stroke by an sLex-glycosylated complement inhibitory protein. *Science* 1999;285:595-599
- 25 33. Connolly ES, Winfree CJ, Stern DM, Solomon RA, Pinsky DJ: Procedural and strain-related variables significantly affect outcome in a murine model of focal cerebral ischemia. *Neurosurg* 1996;38:523-532
- 30 34. Connolly ESJ, Winfree CJ, Springer TA, Naka Y, Liao H, Yan SD, Stern DM, Solomon RA, Gutierrez-Ramos J-C, Pinsky DJ: Cerebral protection in homozygous null ICAM-1 mice after

middle cerebral artery occlusion. Role of neutrophil adhesion in the pathogenesis of stroke. *J Clin Invest* 1996;97:209-216

35. Connolly E, Winfree C, Prestigiacomo C, Kim S, Choudhri
5 T, Hoh B, Naka Y, Solomon R, Pinsky D: Exacerbation of cerebral injury in mice with express the P-selectin gene: identification of P-selectin blockade as a new target for treatment of stroke. *Circ Res* 1997;81:304-310
- 10 36. Bederson JB, Pitts LH, Tsuji M: Rat middle cerebral artery occlusion: evaluation of the model and development of a neurologic examination. *Stroke* 1986;17:472-476

Downloaded from ascelibrary.org by Seattle University on 06/01/15